5-1-2003

Construction of M - Band bandlimited wavelets for orthogonal decomposition

Bryce Tennant

Construction of M – Band Bandlimited Wavelets for Orthogonal Decomposition

by

Bryce Tennant

A Thesis Submitted

in

Partial Fulfillment

of the

Requirements for the Degree of

MASTER OF SCIENCE

In

Electrical Engineering

Approved by:

Prof. R.M. Rao _____
(Thesis Advisor)

Prof. S.A. Dianat _____

Prof. T.M. Rao _____

Prof. V.J. Amuso _____

Prof. R.J. Bowman _____
(Department Head)

DEPARTMENT OF ELECTRICAL ENGINEERING
COLLEGE OF ENGINEERING
ROCHESTER INSTITUTE OF TECHNOLOGY
ROCHESTER, NEW YORK

MAY, 2003

Construction of M – Band Bandlimited Wavelets for Orthogonal Decomposition

Bryce Tennant

May 22, 2003

Permission granted

Title of thesis : Construction of M – Band Bandlimited Wavelets for Orthogonal Decomposition

I, *author's name,* hereby **grant permission** to the RIT Library of the Rochester Institute of Technology to reproduce my thesis in whole or in part. Any reproduction will not be for commercial use or profit.

Date: 07/03/03 Signature of Author _____

Acknowledgements

Thanks are not enough to express the true gratitude that I have for Dr. Raghuveer Rao and all that he has presented to me in my eleven years of working with him. There has been no other person in my life who has had such an incredible effect on my passion for engineering and mathematics.

I would like to thank Adam Templeton, Tom Kenney, Mark Chamberlain, William Furman, Tibor Dobri, and the countless others at Harris Corporation that have provided moral, financial and academic support from day one of my thesis. They are truly exceptional engineers, and I am fortunate to work with all of them on a daily basis.

Without of course my parents, none of this would be possible. I would like to thank my mother for her undying love and support, a gift for which I am forever grateful. To my father, whose work ethic and drive I can only attempt at. I have learned so many things from them both, all of which have gotten me to where I am today.

Special thanks to Greg Smith who has always been my best academic sounding board, our informal technical conversations have always been some of the most enjoyable.

Most importantly, thanks to my loving wife, Julie. Who, second only to myself, has had to make sacrifices to get here. I would like to recognize her for all she has done, every day since we have been together, to so strongly support me with this and all my dreams.

Abstract

While bandlimited wavelets and associated IIR filters have shown serious potential in areas of pattern recognition and communications, the dyadic Meyer wavelet is the only known approach to construct bandlimited orthogonal decomposition. The sinc scaling function and wavelet are a special case of the Meyer. Previous works have proposed a M – Band extension of the Meyer wavelet without solving the problem. One key contribution of this thesis is the derivation of the correct bandlimits for the scaling function and wavelets to guarantee an orthogonal basis. In addition, the actual construction of the wavelets based upon these bandlimits is developed. A composite wavelet will be derived based on the M scale relationships from which we will extract the wavelet functions. A proper solution to this task is proposed which will generate associated filters with the knowledge of the scaling function and the constraints for M-band orthogonality.

Contents

List of Figures

Chapter 1

Introduction

Proper design of M – Band filters for signal decomposition has proved to be one of the most important design problems in the signal processing field in the three decades since their introduction. A proper design promotes the optimal decomposition and reconstruction of a signal into different spectral bands for the analysis of subbands. Encoders that take advantage of the signals characteristic energies can be designed, allowing for a better overall signal representation. Historically, a major difficulty in designing these filters arises primarily due to their non ideal characteristics. Typically M – Band filters generate aliasing that results in a distorted representation of the original signal. It is certainly desired that any distortion introduced by the analysis and synthesis process be minimized or at best, completely eliminated. When considering the design of orthogonal filters, both the magnitude response and phase response need to be closely examined. When decomposing a signal into two bands it has been shown that satisfying both magnitude and phase requirements simultaneously yields a unique set of filters. Although these filters provide for perfect reconstruction, they do not provide for good frequency separation. If one of the conditions is relaxed, many useable two – Band filters can be generated. Quadrature Mirror Filters (QMF) are a set of such a filter banks. Vaidyanathan, Vetterli, Nguyen, and others have shown that a particular set of M – Band

filters, called paraunitary filter banks, can yield perfect reconstruction while maintaining individual filter integrity.

Although the wavelet transform was initially introduced as a more flexible analysis tool for signal representation than the Short Time Fourier Transform, it was quickly linked to the theory of M – Band Filters. The pioneering efforts of Grossman, Morlet, Daubechies, and Meyer allowed for the analysis tool to establish a firm mathematical standing while the groundbreaking works of Daubechies and Mallat provided for a connection between the wavelet transform and subband filtering [39, 40]. Recent works by Gopinath[3], Vetterli[11], Nguyen[35], Selesnick[33], Walter[37] and others have taken the wavelet transform and combined it with the theory of M – Band perfect reconstruction filter banks to generate a powerful signal processing tool. The advantage of the wavelet transform over traditional filters becomes apparent with the spectral characteristics of the transform and the fundamental properties of the resulting basis functions.

The recent works of Vaidyanathan[19], Stedden, Heller, Gopinath, Burrus [3] Vetterli, Herkey [11], and Jones[4] have treated this subject in detail. Typically the resulting M – Band wavelets are generated using polyphase methods or optimization procedures. The results are paraunitary FIR filterbanks that provide for perfect reconstruction. All of these filters offer compact support and therefore result in a frequency response without bound. In contrast, this thesis addresses the problem of designing an orthogonal bandlimited M – Band perfect reconstruction filter bank. This problem was first touched upon in the work of Jones [4] in the context of multi carrier modulation. It will be shown here that the

restrictions he placed on the design of the scaling function are insufficient to guarantee an orthogonal decomposition. We will generate tighter constraints on our scaling function that will result in a new filter bank design and therefore produce very different results.

This thesis will develop the theory of the M – Band wavelet transform and use it to generate a new class of wavelets based on a bandlimited function. In Chapter 2 we will provide a general background on M – Band filter banks and filter theory. Chapter 3 will be dedicated to the introduction of the wavelet transform, the scaling function, mother wavelet and associated filters. We will introduce the theory in the context of a two – Band signal analysis tool. The results will be extended in Chapter 4 so as to develop the theory of the bandlimited orthogonal M – Band wavelet transform. We will develop the constraints and equations that need to be satisfied for the M – Band perfect reconstruction filters, thereby linking the theory introduced in Chapter 2 with that of wavelets. With a firm mathematical foundation provided, we will then proceed to develop our orthogonal bandlimited M – Band scaling function, and wavelets. As a direct result of the development the corresponding filter bank will also be provided. We will introduce the concept of a composite wavelet that will act as a governing shell to all the remaining wavelets embedded within the system once the scaling function has been determined. This section will focus both on the magnitude and the phase response of each derived wavelet. Chapter 5 will illustrate several design examples of the scaling function, wavelets and associated filters for various values of M. We will use on of these results to decompose and reconstruct a signal so as to see the distortion introduced when employing this method.

A brief word on notation. We will commonly replace PR for perfect reconstruction, FT for Fourier transform and QMF for Quadrature Mirror Filters. We will use $\Phi(\omega)$ to represent the scaling function Fourier transform and $\phi(t)$ to represent the time domain equivalent. The corresponding filter to the scaling function will be denoted as $H(\omega)$ with a time domain equivalent of h(n). The M-1 wavelet filter Fourier transforms will be described as $\Psi_m(\omega)$ *where* $m \in \{0,1 \ldots M-2\}$ and $\psi_m(t)$ *where* $m \in \{0,1 \ldots M-2\}$ in the time domain. The corresponding filters for each of these wavelets will be given as $G_m(\omega)$ for the frequency domain representation and $g_m(n)$ for the time domain representation over the same range of m. In some special cases we will substitute $P_i(\omega)$ for the above mentioned filters by letting $P_0(\omega) = H(\omega)$ and $P_i(\omega) = G_{i-1}(\omega)$ for $i \in \{1,2 \ldots M-1\}$.

Chapter 2

General Filter Theory

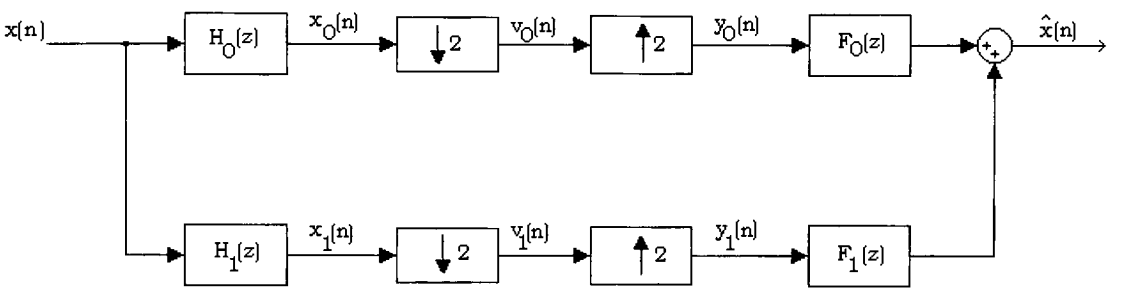

Figure 2.3 - The two – Band decomposition and reconstruction filter bank.

2.1 M – Band Filter Banks

For a two – channel filter bank the general representation for signal decomposition and reconstruction is shown in Figure 2.3. A signal of interest is passed through two separate filters $H_0(\omega)$ and $H_1(\omega)$ corresponding to a low pass and a high pass filter respectively. Each filter output constitutes a frequency band of the input signal. It is clear that if each of the signals bandwidth is half of the input signals bandwidth, the Nyquist sampling theorem implies that we can resample the filtered outputs at half the rate while still maintaining the original signals spectral integrity. However, in practice our filters are never ideal and always contain some energy in the stop band past the cutoff frequency. This implies that when the downsampling of our signal occurs, frequencies greater than the cutoff frequency will be remapped to lower frequencies in our new band. This effect

of aliasing is of primary concern when designing filter banks. The output of these decimators, $v_0(n)$ and $v_1(n)$, are signals that can be encoded or analyzed prior to transmission or storage. When the signal is to be reconstructed, it will be done using a reverse process of expansion. Each subband signal is upsampled and passed through a set of reconstructive filters, $F_0(z)$ and $F_1(z)$. The outputs of these two filters are summed together to get a reconstructed version of the original input signal. Ideally this reconstruction should be a perfect replica of input signal with a possible unit sample shift and constant gain multiplier.

Working backwards from Figure 2.3, we see that the output of the reconstruction portion of the bank is given as

$$\hat{X}(z) = Y_0(z)F_0(z) + Y_1(z)F_1(z)$$

Where both $Y_0(z)$ and $Y_1(z)$ are the outputs of the two interpolators. In the z domain interpolation is given as

$$Y_0(z) = V_0(z^2)$$

providing an output of

$$\hat{X}(z) = V_0(z^2)F_0(z) + V_1(z^2)F_1(z) \qquad \textbf{(2.1)}$$

The $V_n(z)$ terms in (2.1) consists of a primary term that represents the "true" filtered signal and an aliasing term that represents that component of the signal that is greater than the cutoff frequency, ω_c. The signal just prior to the decimator is represented as,

$$X_n(z) = X(z)H_n(z) \text{ where } n \in \{0,1\} \qquad \textbf{(2.2)}$$

The output of any given decimator is the sum of the primary and aliased terms

$$V_n(z) = \frac{1}{2}\left(X\left(z^{1/2}\right)H_n\left(z^{1/2}\right) + X\left(-z^{1/2}\right)H_n\left(-z^{1/2}\right)\right) \text{ where } n \in \{0,1\} \qquad \textbf{(2.3)}$$

Substituting (2.3) back into (2.1) and rearranging allows us to arrive at

$$\hat{X}(z)=\frac{X(z)}{2}(F_0(z)H_0(z)+F_1(z)H_1(z))+\frac{X(-z)}{2}(F_0(z)H_0(-z)+F_1(z)H_1(-z)) \quad \textbf{(2.4)}$$

The second term in equation (2.3) is the aliasing term. It is clear that this term causes distortion in the reconstructed signal and should be eliminated where possible. Using the following notation,

$$T(z)=\frac{F_0(z)H_0(z)+F_1(z)H_1(z)}{2}$$
$$A(z)=\frac{F_0(z)H_0(-z)+F_1(z)H_1(-z)}{2}$$

we can rewrite (2.4) as

$$\hat{X}(z)=X(z)T(z)+X(-z)A(z) \quad \textbf{(2.5)}$$

To completely remove the component of the signal attributed to aliasing we should force the term A(z) in (2.5) to be zero. With this accomplished we are left with the expression $\hat{X}(z)=X(z)T(z)$. Recall that our goal is perfect reconstruction where we have allowed ourselves a constant gain multiplier and some integer sample delay. This implies that our T(z) function must reduce to the form

$$T(z)=c\cdot z^{-n0} \quad \textbf{(2.6)}$$

If we examine real coefficient case of T(z) then we have

$$T(\omega)=c\cdot e^{-j\omega n0} \quad \textbf{(2.7)}$$

The expression given in (2.7) implies that we require a constant multiplier and linear phase to generate perfect reconstruction of our input signal. If in the above system we enforce the following constraints

$$H_1(z) = H_0(-z)$$
$$F_0(z) = H_0(z)$$
$$F_1(z) = -H_1(z)$$

then we have a set of filters that completely satisfy our PR constraints. In addition all analysis and synthesis filters can all be determined from the single prototype filter, $H_0(\omega)$. This form, introduced by Smith and Barnwell in 1986, is commonly referred to as a Quadrature Mirror Filter (QMF). Although by definition a QMF is a set of four filters, the term has become synonymous with any set of M filters that act as an analysis and synthesis pair. Typically they are denoted by the number of channels in the filter bank, or as a M-channel QMF. Such a system is shown in Figure 2.4.

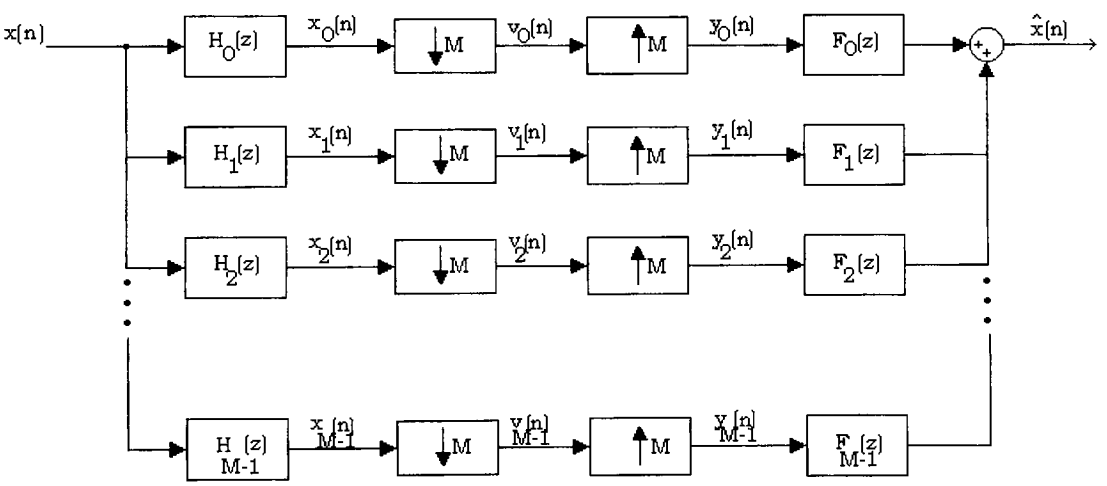

Figure 2.4 - M - Band decomposition and recomposition filter bank

One advantage of this system that does not readily occur in the two – Band case is that perfect reconstruction can be obtained while still designing a filter bank with "good" pass band and stop band characteristics. Vaidyanathan [46] showed that the filter bank in Figure 2.4 can result in perfect reconstruction if certain design criteria are met. Again we

desire the output of the reconstruction filter bank to be a shifted and possibly scaled, version of the filter bank input. To derive the requirements for perfect reconstruction we will start by creating an expression for the m^{th} analysis filter, $H_m(\omega)$, output in terms of the system input. Therefore, for each subband signal prior to the decimation we can write

$$X_m(z) = X(z)H_m(z) \quad where\ m \in \{0,1 \ldots M-1\}$$

The output frequency response of each analysis filter is such that the resulting bandwidth is a factor of M less than the input signals bandwidth. With the signal $X_m(z)$ being bandlimited by π/M, we can pass the result into a decimator that down-samples the signal by a factor of M without any loss in signal integrity. However because we are now decimating into M bands as opposed to two we need to account for the additional alaising terms that are introduced due to the non – ideal nature of the filter $H_m(\omega)$. In the z domain the down-sampling results in a new signal $V_m(z)$ defined as

$$V_m(z) = \frac{1}{M}\sum_{l=0}^{M-1} H_m\left(z^{1/M}W^l\right)X\left(z^{1/M}W^l\right) \quad \text{where we define } W = e^{-j\frac{2\pi}{M}}.$$

In a real world system it is these signals that get encoded for storage or transmission. Figure 2.4 shows the steps required to reconstruct the original signal from the M decimated representations. These signals, $V_m(z)$, are passed through a bank of expanders, up-sampling the signal by a factor of M. Up-sampling essentially inserts M-1 zeros in between each valid sample of $v_m(n)$ to generate new signals $y_m(n)$. The act of up-sampling can be represented in the z domain as

$$Y_m(z) = V_m(z^M) = \frac{1}{M}\sum_{l=0}^{M-1} H_m\left(zW^l\right)X\left(zW^l\right)$$

Each up-sampled signal $Y_m(z)$ is passed through the reconstruction filter $F_m(z)$ to result

in a subband output. The final output of the system is the sum of all the resulting subband signals as shown in (2.8)

$$\hat{X}(z)=\sum_{m=0}^{M-1}F_m(z)Y_m(z)=\frac{1}{M}\sum_{l=0}^{M-1}\left[X(zW^l)\sum_{m=0}^{M-1}F_m(z)H_m(zW^l)\right] \tag{2.8}$$

If we now define a new function $A_l(z)=\sum_{m=0}^{M-1}F_m(z)H_m(zW^l)$ we can simplify (2.8) to be

$$\hat{X}(z)=\sum_{l=0}^{M-1}X(zW^l)A_l(z) \tag{2.9}$$

Clearly the equation in (2.9) allows us to represent the reconstructed output as a function of the original input and M-1 terms of signal aliasing. We can express the sum given in (2.9) as a matrix equation. This allows us to generate an expression in which we can remove each of the undesired aliasing components while enforcing our PR requirements. We will therefore write our definition of $A_l(z)$ as

$$M\begin{bmatrix}A_0(z)\\A_1(z)\\\vdots\\A_{M-1}(z)\end{bmatrix}=\begin{bmatrix}H_0(z) & H_1(z) & \cdots & H_{M-1}(z)\\H_0(zW) & H_1(zW) & \cdots & H_{M-1}(zW)\\\vdots & & \ddots & \vdots\\H_0(zW^{M-1}) & H_1(zW^{M-1}) & \cdots & H_{M-1}(zW^{M-1})\end{bmatrix}\begin{bmatrix}F_0(z)\\F_1(z)\\\vdots\\F_{M-1}(z)\end{bmatrix} \tag{2.10}$$

or in simpler notation

$$\vec{A}(z)=\vec{H}(z)\vec{F}(z) \tag{2.11}$$

where we have absorbed the M scaling factor into our desired A(z). Forcing the appropriate conditions on A in (2.11) allows us to generate a filter bank defined by $H(\omega)$ that is representative of a QMF. We therefore define A(z) such that all aliasing components are identically zero and the only contributing portion of the signal is a result from the unaliased signal input. We therefore write

$$\vec{A}(z)=\begin{bmatrix} MA_0(z) \\ 0 \\ \vdots \\ 0 \end{bmatrix}$$

and solve for the proper unknowns in (2.11) to obtain the final filter design. The H(z) matrix shown in (2.10) is commonly referred to as the Alias Component (AC) matrix.

2.2 Paraunitary Filter Banks

Paraunitary filter banks are a special class of perfect reconstruction filter banks. They have the added benefit of allowing the designer to generate synthesis filters directly from the design of the analysis filters. The causal transfer matrix for a paraunitary filter, H(z), satisfies $\tilde{H}(z)H(z)=cI$ for all z. These conditions come directly from the orthogonal nature of the analysis filters. One useful property of the paraunitary matrix is that for all analysis filters, $[H_0(z)\ H_1(z)\ldots H_{M-1}(z)]$ we have

$$\sum_{k=0}^{M-1}|H_k(\omega)|^2 = c \tag{2.12}$$

This is known as the power complementary (PC) condition and will be pivotal in future sections with the design of our M – Band orthogonal bandlimited wavelet construction. In the dyadic case, the high pass filter can be written as a function of the low pass filter in the analysis filter bank as

$$h_1(n)=(-1)^n h_0^*(L-n) \tag{2.13}$$

The equation given in (2.13) provides us with a method to calculate the high pass filter taps once we are aware of the design of the low pass filter. The synthesis filters can be

found by solving for **F** in (2.11). It can be shown that in the dyadic case the synthesis filters are such that $F_0(z) = z^{-N}\tilde{H}_0(z)$ and $F_1(z) = z^{-N}\tilde{H}_1(z)$ [46]. In the time domain this is represented as the complex conjugate of the mirrored analysis filter, or

$$f_0(n) = h_0^*(L-n) \tag{2.14}$$

$$f_1(n) = h_1^*(L-n) \tag{2.15}$$

Utilizing the paraunitary conditions above an entire two – channel perfect reconstructive system can be built on the premise of (2.13)-(2.15).

Chapter 3

Wavelets

Wavelets have emerged as a powerful field in signal analysis over the past thirty years. Key results introduced by Meyer[27, 40], Daubechies[39], Vetterli[11,42] and many others have allowed this branch of mathematics to grow into a mature field of study. Introduced initially by the Hungarian born Mathematician Aldred Haar, wavelets started out as a strictly mathematical curiosity. Published as an appendix in his doctoral thesis, Haar showed that a dilated and shifted function could generate orthogonal systems of functions. It was not until the mid seventies, while working at an oil company, did Jean Morlet actually formally develop the theory of wavelets. He developed the theory to overcome the shortcomings of the STFT. Morlet was the first to generate a "mother wavelet" and apply the theory to analyze signals using multi-resolution analysis. Working with Alex Grossman the two showed that the transform could decompose a signal and recompose it while maintaining signal integrity. This was a critical step in the development of the wavelet theory. The multi-resolution theory of wavelets was formally developed by Meyer and Mallat in the late 1980s. This provided further theory for developing specific wavelets and scaling functions based on the application of interest. It was not until Ingrid Daubechies made the connection between wavelets and filter bank theory did the transform become the useful to signal processing.

In their most basic form, wavelets are signal analysis tools, similar to Fourier analysis, that decompose a signal into spectral components. The wavelet transform is unlike its Fourier transform cousin, in that it provides time domain information while also providing for frequency content. Unlike the Fourier's $e^{-j\omega t}$, the wavelet transform does not have predefined basis functions. Instead wavelets and scaling functions are designed as orthogonal functions based on a strict set of rules that, in the end, govern the shape of each function. Determining a wavelet basis has proved to be a fairly difficult task. Daubechies developed a set of rules that can be applied to generate wavelets with compact support[39]. Meyer applied the rules to generate some of the first known bandlimited wavelet functions[40], which are of particular interest to this thesis development. There is abundant literature available in this area, interested readers are referred to the works [2][3][31]-[38],[39]-[43].

3.1 Basic Wavelet Theory

The wavelet, $\psi(t)$, is defined as a continuous time function with zero mean and finite energy. Expressed in mathematical notation, this function therefore must satisfy the conditions imposed in both (3.1) and (3.2) below.

$$\int_{-\infty}^{\infty} \psi(t)dt = 0 \tag{3.1}$$

$$\int_{-\infty}^{\infty} |\psi(t)|^2 = c \quad where\ c < \infty \tag{3.2}$$

These conditions create functions that are oscillatory in nature and tend to zero as t

approaches infinity. In addition wavelets must satisfy the so called Admissibility Condition in (3.3). The condition guarantees that any wavelet transform will have an inverse, allowing the developer to completely reconstruct the signal from the signal decomposition. The $\Psi(\omega)$ term is the frequency response of the wavelet function.

$$\int_{-\infty}^{\infty} \frac{|\Psi(\omega)|^2}{|\omega|} \equiv C \tag{3.3}$$

Wavelet and scaling functions can be either bandlimited or can have compact support in time. These two possibilities result in functions that behave differently and have advantages and disadvantages in implementation. The literature found throughout this field typically focuses on compactly supported wavelets. This is primarily due to the well-understood and simple means of FIR filter implementation. These filter implementations, however, do have a pitfall due to their compactly supported nature. They will have an infinite frequency response, causing signal leakage into the designed filters stop band. In addition these wavelets tend not to have smooth band edges and can result in choppy looking functions. This phenomenon can clearly be seen when examining any of the Daubechies wavelet functions. The alternative approach is to utilize a bandlmited wavelet. This results in a smooth function that does not pass signal into the filters stop band. The clear disadvantage is in the complexity of the filter implementation due to the IIR nature of the inverse Fourier transform. Figure 3.1 provides one possible bandlimited wavelet function commonly referred to as the Meyer wavelet. In order to maintain orthogonality of the scaling function and wavelet, very tight rules must be

applied to the function in the frequency domain that governs the pass band, stop band and transition band of the scaling functions Fourier transform.

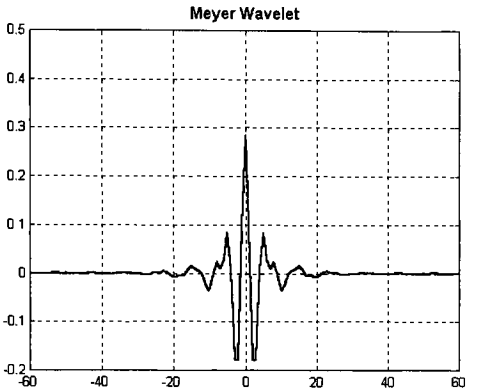

Figure 3.1 - The time domain representation of the Meyer Wavelet

Like the Fourier transform, the wavelet transform uses a set of basis functions to decompose a signal into its constituent parts. These basis functions form a tight frame[39,40]. For our purposes we will define a tight frame to be a set of functions such that any f(t) can be composed using the functions that span the tight frame. The function f(t) will be generated using a weighted sum of the basis functions where the weights are determined as the projection of the basis functions with the function f(t) itself. Because wavelets form a nested subspace the transform must be expressed in terms of dilated versions of a single prototype function, commonly referred to a the mother wavelet. Conceptually the transform dilates and shifts this function, $\psi(t)$, by factors a and b respectively. When a function f(t) is projected onto these dilated functions the result is a two dimensional time – frequency analysis.

$$W(a,b)=\frac{1}{\sqrt{a}}\int_{-\infty}^{\infty} f(t)\psi^*\left(\frac{t-b}{a}\right)dt \tag{3.4}$$

From (3.4) we see that our wavelet basis functions are defined as

$$\psi_{a,b}(t)=\frac{1}{\sqrt{a}}\psi\left(\frac{t-b}{a}\right) \tag{3.5}$$

The constant factor $\frac{1}{\sqrt{a}}$ in each basis function is present so as to normalize the analysis function to unit energy. Substituting (3.5) back into the definition of the transform we get a final expression for the continuous wavelet transform.

$$W(a,b)=\frac{1}{\sqrt{a}}\int_{-\infty}^{\infty} f(t)\psi^*_{a,b}(t)dt \tag{3.6}$$

The variables of the transform, a and b, control the dilation and shift amount of the mother wavelet respectively. It is these two parameters that provide for the time-frequency representation offered by the wavelet transform. If our wavelet satisfies the admissibility condition in (3.3) then we can define the inverse wavelet transform as

$$f(t)=\frac{1}{C}\int_{a=-\infty}^{\infty}\int_{b=-\infty}^{\infty}\frac{1}{|a|^2}W(a,b)\psi_{a,b}(t)da\,db \tag{3.7}$$

where C is the constant defined in (3.3).

3.2 The Discrete Wavelet Transform

The continuous transform that is described above fits nicely into a situation where we want to visualize the structure of a signal. It does not however readily lend itself to digital signal processing. Daubechies showed that the redundancy of the continuous transform

can be removed and a discrete time equivalent can be developed [39]. We start by defining a new function $\phi(t)$ which must satisfy the following properties

$$\int_{-\infty}^{\infty} \phi(t)dt = 1$$

$$\|\phi(t)\|^2 = \int_{-\infty}^{\infty} |\phi(t)|^2 dt = 1$$

$$\langle \phi(t), \phi(t-n) \rangle = \partial(n)$$

This new function, called the scaling function, must have unit energy and be orthogonal to integer translates of itself. This implies that each translate is linearly independent and the set $\{\phi(t-n)\}$ where n is an integer, forms a basis for a linear vector space. We will denote this vector space as V_0. If we dilate the scaling function by a factor of 2^{-k} we generate,

$$\langle \phi(2^{-k}t), \phi(2^{-k}t-n) \rangle = 2^k \partial(n) \qquad \textbf{(3.8)}$$

Equation (3.8) defines a linear vector space, V_k. This dilation implies that for increasing k the corresponding vector space, V_k, generates coarser and coarser approximation of $L^2\{R\}$. Hence for any function f(t) that resides within V_k, f(2t) must completely be contained within V_{k-1}. If we further define the vector space such that every vector in V_k must also be in V_{k-1}, then we can write the basis function $\phi(t)$ in terms of a linear combination of basis functions of the next finer level. More concisely, if $V_0 \subset V_{-1}$ then we can write

$$\phi(t) = \sum_{n=-\infty}^{\infty} c(n)\phi(2t-n) \tag{3.9}$$

We now develop a frequency domain representation of the results provided in (3.9). It was defined that our scaling function must satisfy the following orthogonality constraint

$$\langle \phi(t), \phi(t-n) \rangle = \partial(n) \tag{3.10}$$

Taking the FT of (3.10) results in the commonly referred to Poisson summation formula shown in (3.11)

$$\sum_{l=-\infty}^{\infty} \left| \Phi(\omega + 2\pi l) \right|^2 = 1 \tag{3.11}$$

This formula will be used in many locations through out the remainder of our development and should be noted as a direct result of the orthogonality constraint placed on our basis functions $\phi(t)$. We will now show if we satisfy the orthogonality constraints on the scaling function and if $\{\phi(t-k)$: for k integer$\}$ forms a nested subspace [40], then the c(n) in (3.9) satisfies the power complementary condition given in (2.12). We define the Fourier transform of the discrete sequence c(n) as

$$C(\omega) = \sum_{n=-\infty}^{\infty} c(n) e^{-j\omega n} \tag{3.12}$$

If we let $t = \frac{\tau}{2}$ and substitute this into (3.9) we arrive at

$$\phi\left(\frac{\tau}{2}\right) = \sum_{n=-\infty}^{\infty} c(n)\phi(\tau - n) \tag{3.13}$$

which has a FT of

$$2\Phi(2\omega) = C(\omega)\Phi(\omega) \tag{3.14}$$

The discrete nature of c(n) results in the function $C(\omega)$ being 2π periodic. Shifting the results in (3.14) by an amount $2\pi k$ results in

$$2\Phi(2\omega + 4\pi k) = C(\omega + 2\pi k)\Phi(\omega + 2\pi k) \tag{3.15}$$

Taking the magnitude squared of both sides and summing over k gives

$$4\sum_k |\Phi(2\omega + 4\pi k)|^2 = |C(\omega)|^2 \sum_k |\Phi(\omega + 2\pi k)|^2 \tag{3.16}$$

The summation on the right-hand side of (3.16) is nothing more than the Poisson Summation formula defined in (3.11) reducing the expression to

$$4\sum_k |\Phi(2\omega + 4\pi k)|^2 = |C(\omega)|^2 \tag{3.17}$$

We now make the substitution of $\omega' = \omega + \pi$ and distribute this through (3.17)

$$4\sum_k |\Phi(2\omega' + 2\pi + 4\pi k)|^2 = |C(\omega' + \pi)|^2 \tag{3.18}$$

If we add both (3.17) and (3.18) together we get

$$4\sum_k |\Phi(2\omega + 4\pi k)|^2 + 4\sum_k |\Phi(2\omega + 2\pi + 4\pi k)|^2 = |C(\omega)|^2 + |C(\omega + \pi)|^2 \tag{3.19}$$

Close examination reveals that the two summations on the left-hand side of (3.19) are nothing more that the even and odd terms of k in the Poisson summation formula reducing (3.19) to our final form of

$$4 = |C(\omega)|^2 + |C(\omega + \pi)|^2 \tag{3.20}$$

3.3 Approximation of a Signal f(t) with Scaling Function $\phi(t)$

In the above section we have developed an orthogonal set of basis functions that will approximate any function in $L^2\{R\}$. We will now use this $\phi(t)$ to approximate an arbitrary function f(t). We start by assuming knowledge of a set of coefficients a(k,n) such that for some decomposition level k

$$f_k(t) = \sum_{n=-\infty}^{\infty} \phi(2^{-k}t - n)a(k,n) \tag{3.21}$$

Therefore at some arbitrary resolution k and the previous coarser resolution k+1, we define the difference between these two approximations as the detail lost in transitioning from the finer space to the coarser space. This is the same as projecting the finer approximation $f_k(t)$ onto space V_{k+1}. We transition from signal space V_k to signal space V_{k+1} with some error signal defined as $g_{k+1}(t) = f_k(t) - f_{k+1}(t)$. The error, $g_{k+1}(t)$, is contained completely within the signal space V_k and is orthogonal to the signal $f_{k+1}(t)$. It would be plausible to reconstruct some signal $f_k(t)$ be retaining a single course approximation and a series of detail functions captured when moving from vector space V_n to V_{n+1}. We will define the wavelet function $\psi(t)$ that will be used to capture the detail lost when moving to a coarser subspace. This wavelet function, as with the scaling function, must obey some simple rules of construction. Firstly it must integrate to zero

$$\int_{-\infty}^{\infty} \psi(t)dt = 0$$

In addition the wavelet must have unit energy

$$\int_{-\infty}^{\infty} |\psi(t)|^2 dt = 1 \tag{3.22}$$

and its integer translates must be orthogonal to shifted versions of itself.

$$\langle \psi(t), \psi(t-n) \rangle = \partial(n) \tag{3.23}$$

An additional constraint is that this new function must also be orthogonal to shifted versions of the scaling function. This is because $\psi(t)$ exists completely within the previous finer signal space from $\phi(t)$.

$$\langle \psi(t), \phi(t-n) \rangle = 0 \tag{3.24}$$

Equation (3.24) allows us to define ψ(t) in terms of translates of the scaling function in the previously finer domain.

$$\psi(t) = \sum_{n=-\infty}^{\infty} d(n)\phi(2t-n) \tag{3.25}$$

The coefficients, d(n), satisfy similar properties to those in the scaling function definition and using similar development as in (3.20) we can write d(n) in the frequency domain as

$$|D(\omega)|^2 + |D(\omega+\pi)|^2 = 4 \tag{3.26}$$

The orthogonal nature of equation (3.24) along with the definitions in (3.20) and (3.26) let us write a final equation relating the two frequency responses C(ω) and D(ω)

$$C(\omega)D^*(\omega) + C(\omega+\pi)D^*(\omega+\pi) = 0 \tag{3.27}$$

where the * denotes the complex conjugate. The results of (3.20), (3.26) and (3.27) can be combined into one compact matrix equation.

$$\begin{bmatrix} C(\omega) & C(\omega+\pi) \\ D(\omega) & D(\omega+\pi) \end{bmatrix} \begin{bmatrix} C^*(\omega) & D^*(\omega) \\ C^*(\omega+\pi) & D^*(\omega+\pi) \end{bmatrix} = 4I \tag{3.28}$$

The commutative nature of (3.28) provides us with a mechanism to swap the order of the matrix multiplication without affecting the integrity of the result

$$\begin{bmatrix} C^*(\omega) & D^*(\omega) \\ C^*(\omega+\pi) & D^*(\omega+\pi) \end{bmatrix} \begin{bmatrix} C(\omega) & C(\omega+\pi) \\ D(\omega) & D(\omega+\pi) \end{bmatrix} = 4I \tag{3.29}$$

Equation (3.29) defines our system in detail and provides some interesting implications that relate the theory of wavelets to that of filter banks. If we look back to the previous section on M – Band filtering we see that the above equation defines a paraunitary filter bank. This implies that the two functions C(ω) and D(ω) are actually low pass and high pass filters respectively. This follows our intuition as the C(ω) is developed from the

approximation function and the D(ω) is developed from the detail information. Typically low pass filtering provides an approximation or averaging of the original signal whereas the high pass filtering preserves the signals detail information. From (3.29) we can write three filtering equations found in (3.30)-(3.32).

$$|C(\omega)|^2 + |D(\omega)|^2 = 4 \tag{3.30}$$

$$|C(\omega+\pi)|^2 + |D(\omega+\pi)|^2 = 4 \tag{3.31}$$

$$C(\omega)C^*(\omega+\pi) + D(\omega)D^*(\omega+\pi) = 0 \tag{3.32}$$

For our development we will define two new functions h(n) and g(n) which are simply

$$h(n) = \frac{c(n)}{2}$$
$$g(n) = \frac{d(n)}{2} \tag{3.33}$$

This simplifies our formula in (3.27),(3.30),(3.31) to

$$|H(\omega)|^2 + |G(\omega)|^2 = 1 \tag{3.34}$$

$$|H(\omega+\pi)|^2 + |G(\omega+\pi)|^2 = 1 \tag{3.35}$$

$$H(\omega)G^*(\omega) + H(\omega+\pi)G^*(\omega+\pi) = 0 \tag{3.36}$$

We have defined a complete QMFB that satisfies the paraunitary condition. This implies that if we create a prototype filter H(ω) from a valid scaling function ϕ(t) then we can quickly determine the analysis and synthesis filters H(ω) as a prototype function. A simple table is provided below to illustrate the development of the analysis and synthesis filters. The analysis filters are in the first column and the corresponding synthesis filters are in the second column. The only filter that needs to be determined using the governing rules is the scaling filter h(n). The remaining three filters fall out directly as a result of the paraunitary conditions.

	Analysis Filters	Synthesis Filters
Low Pass	$h(n)$ determined by governing rules of scaling function.	$\tilde{h}(n) = h(-n)$
High Pass	$g(n) = (-1)^{1-n} h(1-n)$	$\tilde{g}(n) = g(-n)$

We can now reduce the process of performing the wavelet transform to a technique of low pass and high pass filtering. As discussed in the section on general filter banks, we can down-sample the signal output of a filter whose bandwidth is half of the original signals bandwidth by a factor of two without loss of signal information. If we apply the scaling filter and wavelet filter, as shown in Figure 3.2, we can follow the filtering with a decimation. This generates a course approximation, $a_1(n)$ and a detail function, $d_1(n)$. The low pass approximation is then passed through the same bank of filters and again decimated. This process continues until the desired resolution is reached. The end result is a series of detail functions and a single coarse approximation function. The reverse process is used to recombine the signal from its constituent parts. A schematic of the analysis and synthesis banks are found in Figure 3.2.

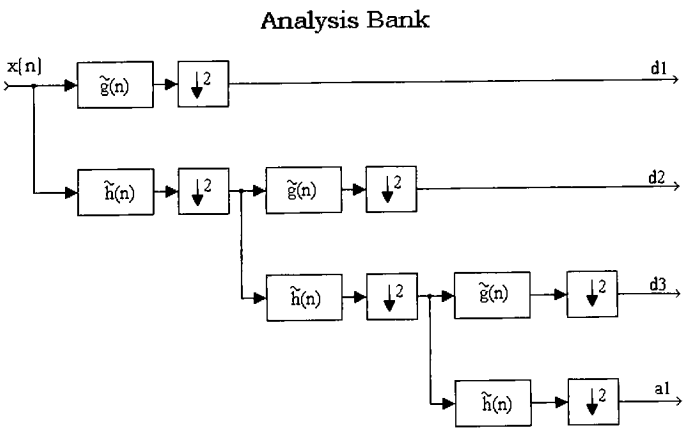

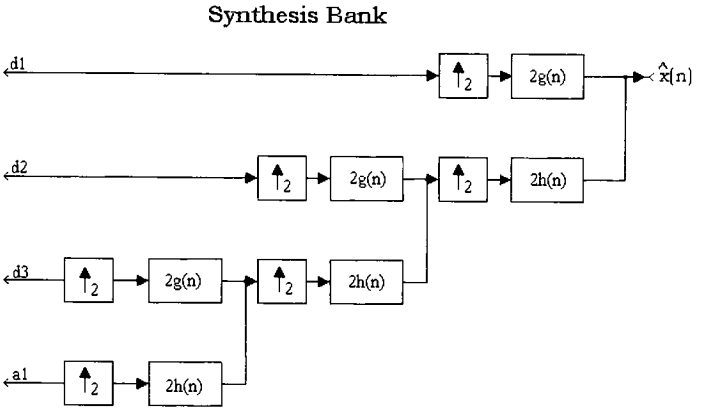

Figure 3.2 - Analysis and synthesis wavelet filter banks

3.4 Bandlimited Wavelets

Typically wavelets developed for signal processing have compact support in time resulting in FIR filters. Many recent papers have been written on the development of FIR wavelet filter banks[5][9-10][12-13],[32],[34]. The Daubeichies wavelet has become one of the most recognized wavelets in the signal processing community. This wavelet and scaling function, seen in Figure 3.3, results in a compactly supported filter, clearly implying that the frequency response is without bound. The frequency response of the Daubechies scaling function and wavelet can be seen in Figure 3.4. Compactly supported filters will always result in aliasing due to the impulse response of the filter.

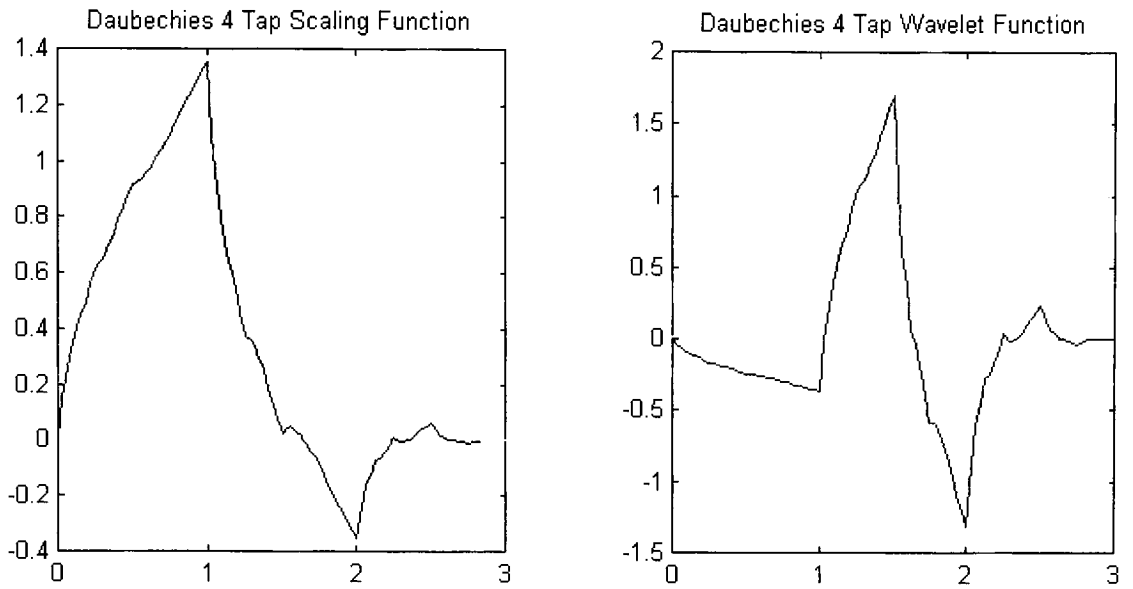

Figure 3.3 - The Daubechies 4 tap scaling function and wavelet in time

Depending on the application, the smoothness of the wavelet can be critical in the implementation of the design. A smooth wavelet helps isolate edges and features in a signal. We tend to desire wavelets that have some degree of smoothness over those that appear chaotic by nature. One common metric of smoothness is the Hölder exponent [43] which is essentially a measurement of local differentiability. We can conclude that the four tap Daubechies wavelet has a low Hölder exponent and is actually differentiable only once. The implication is that there is a slow decay in the frequency domain which does not allow for frequency localization of events. Although there are many Daubechies wavelets of varying lengths, we need a large number of filter taps to generate a smooth wavelet that is M times differentiable. Our design will focus on wavelets that are infinitely differentiable and therefore smooth by definition.

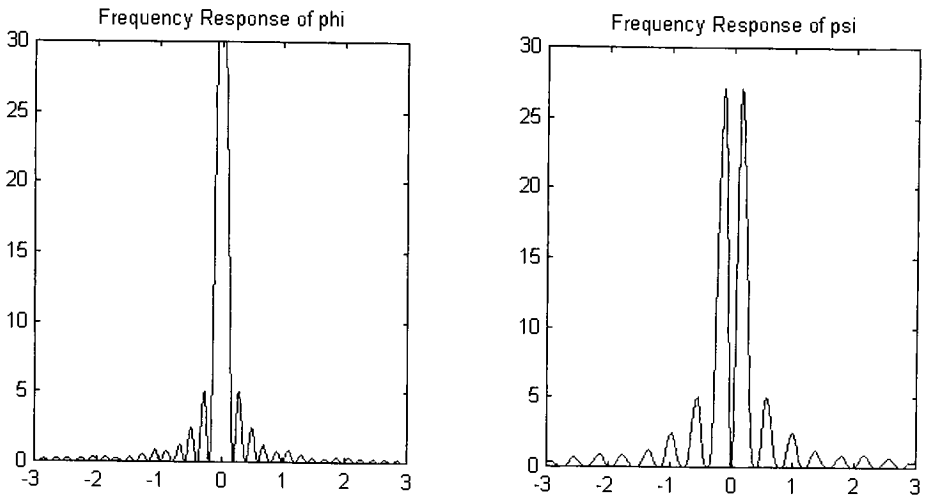

Figure 3.4- Magnitude frequency response of the Daubechies four tap scaling function and wavelet.

3.5 The Meyer Wavelet

The Meyer wavelet is a continuous time wavelet that is band-limited over the range $0 \leq \omega \leq 4\pi/3$. This band limitedness causes the wavelet to be IIR, but despite this apparent disadvantage, the filter is practical and offers both good time and frequency resolution [2]. The Meyer wavelet has also been shown to be closely related to the raised cosine function prominent in communications [31][37]. This naturally leads to designs in communication systems that take advantage of this relationship. W.W. Jones proposed a M – Band filter based on the Meyer wavelet that was used for orthogonally multiplexed communications or multi carrier modulation. Rao, Bopardikar, and Adiga [1] showed that the Meyer wavelet naturally arises in subsampled bandlimited processes. They illustrated that the reconstruction filter banks can optimally recreate a sub sampled bandlimited signal if the resultant samples are passed through a filter that is derived from a Meyer

wavelet. It is also well known that in communication systems that a filter can provide for optimum signal detection and energy compaction when the filters spectrum is matched to that of the signal that is being detected. Rao and Chapa further illustrated in [2] that the bandlimited Meyer wavelet can be directly designed to optimally match the magnitude and phase of a known signal while still preserving the wavelets orthogonality. A detailed development of the Meyer wavelet and scaling function can be found in their paper, primary results that pertain to this work are reproduced below.

We start by defining the half band of the scaling function as being the positive bandwidth of the frequency response $\Phi(\omega)$, which clearly must be less than π. Therefore, it must be that the half band of $|\Phi(2\omega)| \leq \pi$. The Poisson Summation formula in (3.11) reduces to be

$$|\Phi(\omega)|^2 + |\Phi(\omega + 2\pi)|^2 = 1 \quad for \quad 0 \leq \omega \leq 2\pi \tag{3.37}$$

If the half band frequency of $\Phi(\omega)$ is defined to be ω_m, then from our discussion above $\omega_m \geq \pi$. If we define the excess bandwidth that is greater than π as α we can write

$$\omega_m = \pi + \alpha \tag{3.38}$$

where $\alpha \geq 0$. Utilizing the reduced Poisson Summation formula given in (3.37) we can see that the bandlimited nature of the scaling function forces us to write the following restrictions on $\Phi(\omega)$ to satisfy the summation.

$$\begin{cases} |\Phi(\omega)|^2 = 1 \quad for \; |\omega| \leq (\pi - \alpha) \\ |\Phi(\omega)|^2 + |\Phi(\omega - 2\pi)|^2 = 1 \quad for \; (\pi - \alpha) \leq |\omega| \leq (\pi + \alpha) \end{cases} \tag{3.39}$$

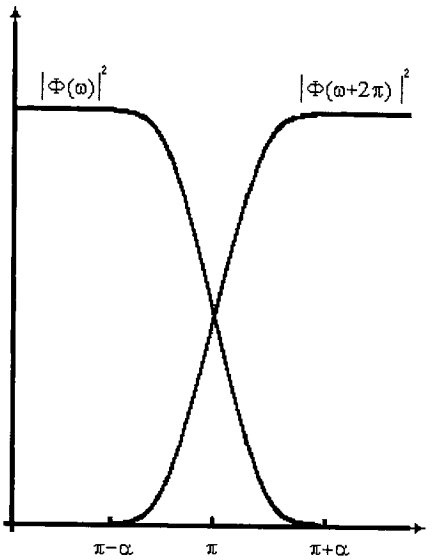

Figure 3.5- Meyer wavelet frequency response The structure is above is defined as a result of the Poisson summation formula

Figure 3.5 illustrates how these two functions overlap and interact with one another to enforce the results in (3.39). Combining the results from both (3.14) and (3.33) it is easy to show that

$$H(\omega)=\frac{\Phi(2\omega)}{\Phi(\omega)} \tag{3.40}$$

This equation allows us to develop the frequency response of the associated low pass filter with the knowledge of the frequency response of the scaling function, $\Phi(\omega)$. Knowing that $\Phi(2\omega)$ is a compressed version of $\Phi(\omega)$, we can generate regions of support for the filter $H(\omega)$ with the definition in (3.40). Recall that h(n) is a discrete time filter, which implies that the frequency response, $H(\omega)$, is 2π periodic. Because the dilated frequency response, $\Phi(2\omega)$, goes to zero at $\omega_m+\alpha$ the filter must obey

$$H(\omega)=0 \; for \; \omega \geq \frac{\pi+\alpha}{2}$$

The periodic nature of the filter, H(ω), allows us to write

$$H\left(2\pi-\frac{\omega+\alpha}{2}\right)=H\left(\frac{3\pi-\alpha}{2}\right)=0 \tag{3.41}$$

Graphically we show these two periods of H(ω) as follows

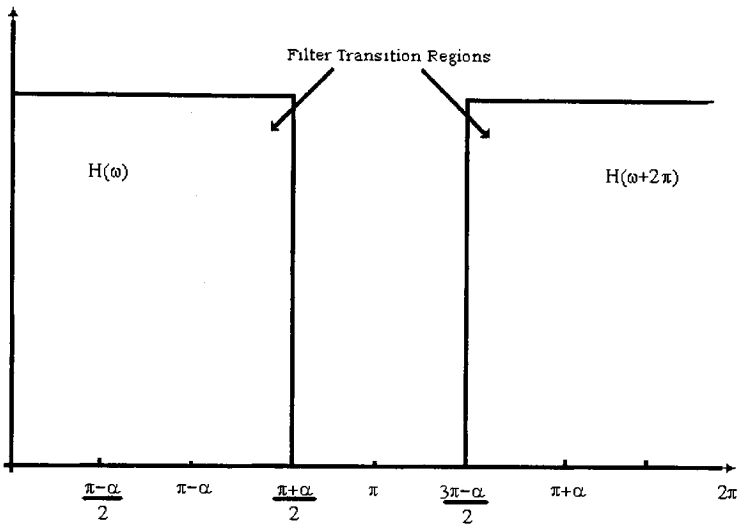

Figure 3.6- Regions of support for the Meyer low pass filter. Gray regions represent regions of transition from pass band to stop band.

Limiting ourselves to the range $0<\omega<2\pi$ we see the filter H(ω) is exactly zero in the region $\frac{\pi+\alpha}{2} \leq \omega \leq \pi+\alpha$ and the shifted version is identically zero in the range defined by $\pi-\alpha \leq \omega \leq \frac{3\pi-\alpha}{2}$. If we take the best case scenario where these two bands coincide we see that

$$\frac{\pi+\alpha}{2}=\pi-\alpha$$

Solving for α gives us a maximum value that is acceptable to satisfy these periodic

conditions

$$\alpha = \frac{\pi}{3} \tag{3.42}$$

This value is absolutely crucial to the development of the Meyer wavelet and will prove to be even more important when we expand our development to the M – Band case. Any value of α that exceeds this will cause filter overlap and violate the rule dictated by (3.26). It should be noted that the Poisson Summation formula operates only on the magnitudes of the scaling function and places no restrictions on the phase of the solution. This implies that a phase solution to the scaling function needs to be developed as a separate step in the development process. Now that a limitation has be derived for the α term, a scaling function can be generated directly from the results in (3.39). The design now reduces to determining appropriate transition bands that satisfy the Poisson summation formula, graphically depicted in Figure 3.6. We can do this by finding a function $f(\omega)$ and $g(\omega)$ such that

$$f(\omega)^2 + g(\omega)^2 = 1$$

and

$$g(\omega)^2 = f(2\pi - \omega)^2 \ \ in\ region\ \ (\pi - \alpha) \le \omega \le (\pi + \alpha)$$

Further development in [2] shows that the corresponding wavelet in the two band case is defined as

$$|\Psi(\omega)|^2 = \begin{cases} 0, & for \quad 0 \le \omega \le (\pi - \alpha) \\ g(\omega), & for \quad (\pi - \alpha) < \omega \le (\pi + \alpha) \\ 1, & for \quad (\pi + \alpha) < \omega \le (2\pi - 2\alpha) \\ f\left(\frac{\omega}{2}\right), & for \quad (2\pi - 2\alpha) < \omega \le (2\pi + 2\alpha) \\ 0, & for \quad w \le (2\pi + 2\alpha) \end{cases} \tag{3.43}$$

The FT of the wavelet defined in (3.43) is shown in the figure below. Make notice of the locations of the 3dB points in this figure as it becomes necessary to utilize this in subsequent sections of the M – Band design.

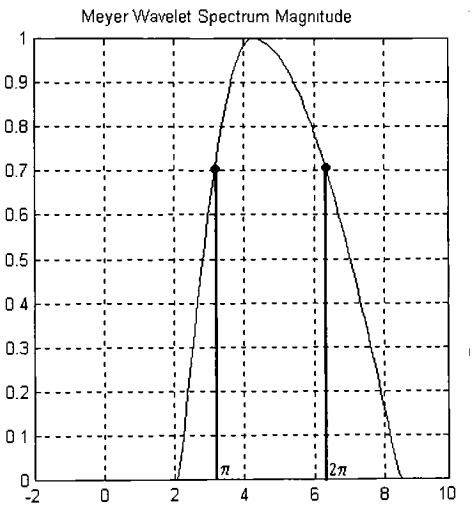

Figure 3.7- The Meyer wavelet spectrum magnitude. Notice the 3dB points occur at π and 2π respectively.

As in (3.40) there is a corresponding filter equation for the wavelet ψ(t). If we take the FT of the two scale relationship found in (3.25) we get an equivalent frequency domain representation

$$2\Psi(2\omega) = D(\omega)\Phi(\omega) \tag{3.44}$$

This in conjunction with the definition of the function g(n) in (3.33) provides an expression for the wavelets filter as

$$G(\omega) = \frac{\Psi(2\omega)}{\Phi(\omega)} \tag{3.45}$$

The above development does not illustrate the phase solution of the wavelet. This is covered in detail for the dyadic case in [2].

Chapter 4

M – Band Wavelet Development

We now have developed much of the foundation that is required for the M – Band wavelet design. We have illustrated the basic principles that govern M – Band filter theory and the theory for wavelet analysis. A synthesis routine for the Meyer scaling function, wavelet function and the corresponding filters have been presented. We will now generate a M – Band wavelet filter bank based on a non-trivial extension of the results in the previous sections. We will first develop the magnitude response for the scaling function and wavelets in similar way that was presented above. Once the Poisson summation formula has been appropriately satisfied, we will generate phasing details for the corresponding wavelets so as to maintain orthogonality across all filters.

4.1 M – Band Theory of Wavelets

Assume that we are given some signal, $f(t) \in V_{-\infty}$, that we wish to break up into M separate banks. It is desirable that the original filtered signal can be reconstructed without error due to aliaising or amplitude distortion. We know that V_k is the space that contains the vectors to approximate f(t) as $f_k(t)$. We have also illustrated that V_{k-1} is the next finer

detailed space to V_k. If we define W_k as the detail lost in going from V_{k-1} to V_k then we can write

$$V_k = \bigoplus_{j=k}^{\infty} W_j \tag{4.1}$$

and $W_k \in V_{k-1}$. Here we have used W_k to represent the total detail lost in moving from a finer resolution to the next coarser one. There are however M-1 bands of detail space that we need to consider. Each band will contain some detail information about the original signal that will need to be captured when translating from V_{k-1} to V_k. Rewriting (4.1) to account for this generates

$$V_k = \bigoplus_{m=0}^{M-2} \bigoplus_{j=k}^{\infty} W_{m,j} \tag{4.2}$$

We have used m to represent the detail space in question. This implies that there are M-1 signals that need to be determined in order to capture all the detail lost when performing this projection. We will denote these signals as $e_{k,m}(t)$ where k is the level of the decomposition and m represents the band that we are decomposing. These functions represent the signal lost in each band when the transform is made. A simple symbolic diagram is shown in Figure 4.1 and capture this.

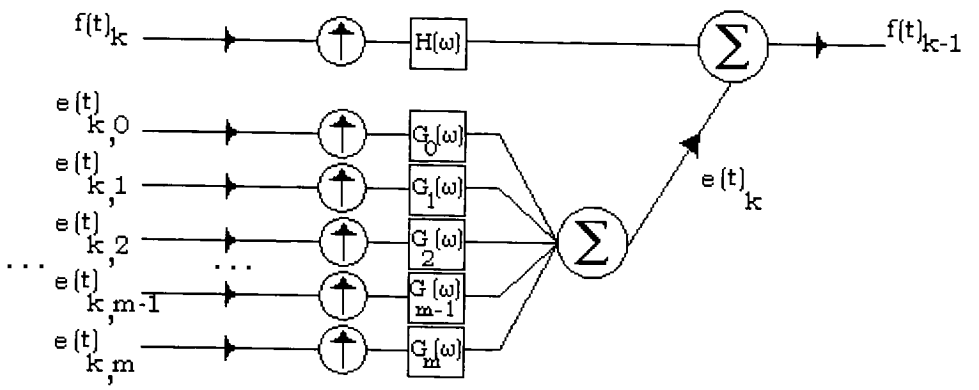

Figure 4.1 - M - Band details and approximation $f(t)_k$ used to generate the next finer resolution approximation of f(t)

We let $\phi(t)$ be the scaling function and $\psi_m(t)$, m=0,1,...M-2, be the wavelets in a M – Band orthogonal decomposition. For M – Band systems the scaling function, $\phi(t)$, is designed to be orthogonal to integer translates of itself across all scales. This implies

$$\langle \phi(t), \phi(t-n) \rangle = \partial(n) \tag{4.3}$$

Taking the Fourier Transform of (4.3), provides the well known Poisson summation formula.

$$\sum_k |\Phi(\omega + 2\pi k)|^2 = 1 \qquad -\infty < k < \infty \tag{4.4}$$

To generate a multi-resolution decomposition, we must allow for $\phi(t)$ to be reconstructed from integer shifts from the previous finer resolution

$$\phi(t) = \sum_{n=-\infty}^{\infty} c(n)\phi(Mt - n) \tag{4.5}$$

for scalars, $c(n)$, $n \in Z$. This becomes in the frequency domain

$$M\Phi(M\omega) = C(\omega)\Phi(\omega) \tag{4.6}$$

Where $C(\omega) = \sum_{n=-\infty}^{\infty} c(n)e^{-j\omega n}$ and $\Phi(\omega)$ is the FT of $\phi(t)$. The corresponding equation for the M-1 wavelets and their associated filters can be found using the same principles

$$M\Psi_m(M\omega) = D_m(\omega)\Phi(\omega),\ m = 0,1\ldots M-2 \tag{4.7}$$

These relationships, referred to as the 2 – Scale relationships, relate the FT's of the scaling function and wavelets, namely $\Phi(\omega)$ and $\Psi_m(\omega)$, to the digital filter frequency responses, $C(\omega)$ and $D_m(\omega)$ respectively. For our development we normalize the filters by defining

$$h(n) = \frac{c(n)}{M} \qquad g_m(n) = \frac{d_m(n)}{M} \tag{4.8}$$

We will now use the results of the previous sections to show

$$\sum_{m=0}^{M-1}\left|H\left(\omega + \frac{2\pi m}{M}\right)\right|^2 = 1 \tag{4.9}$$

We start with the results in (4.6), simplified with the use of (4.8), and substitute in the expression $\omega = \omega + 2\pi k$. Taking the magnitude squared of the result and summing both sides over k we obtain

$$\sum_k \left|\Phi(M\omega + 2\pi Mk)\right|^2 = \left|H(\omega)\right|^2 \sum_k \left|\Phi(\omega + 2\pi k)\right|^2 \tag{4.10}$$

The result on the left hand side of (4.10) can be simplified using the Poisson summation formula,

$$\sum_k \left|\Phi(M\omega + 2\pi Mk)\right|^2 = \left|H(\omega)\right|^2 \tag{4.11}$$

We also know from the Poisson summation formula that

$$\sum_k \left|\Phi(M\omega + 2\pi k)\right|^2 = 1 \tag{4.12}$$

Returning to (4.11) we see that this equation provides us with the $2\pi kM$ terms (0, $2\pi M$, $4\pi M\ldots$) of (4.12). If we substitute $\omega = \omega + \pi$ into (4.11) we arrive at

$$\sum_k \left|\Phi(M\omega + M\pi + 2\pi Mk)\right|^2 = \left|H(\omega + \pi)\right|^2 \tag{4.13}$$

This expression provides the terms, πM, $3\pi M$, $5\pi M$ and so forth. This process is repeated

for all $\omega_m = \frac{2\pi m}{M}$ $m \in \{0 \ldots M-1\}$. Summing the resultant M expressions together gives

$$\sum_k \left|\Phi(M\omega + 2\pi k)\right|^2 = \sum_{m=0}^{M-1} \left|H\left(\omega + \frac{2\pi m}{M}\right)\right|^2 \quad \textbf{(4.14)}$$

Recognizing that the first summation is nothing more than what we presented in (4.12) provides us with the result that we set out to prove in (4.9).

Similar methods can be used to provide equivalent results for the wavelet functions and filters frequency responses, $\Psi_m(\omega)$ and $G_m(\omega)$. Unlike the two – Band case where there is a single scaling function and a corresponding wavelet, the M – Band system has M-1 wavelet functions that we will reference as $\Psi_m(\omega)$ where $m \in \{0,1 \ldots M-2\}$. The results that we obtain for the wavelet filters $G_m(\omega)$ are

$$\sum_{p=0}^{M-1} \left|G_m\left(\omega + \frac{2\pi p}{M}\right)\right|^2 = 1 \quad where\ m \in \{0,1 \ldots M-2\} \quad \textbf{(4.15)}$$

Finally we are interested in how the scaling filter and each wavelet filter interact with one another in the frequency domain. We know that each wavelet function can be expressed as a weighted sum of the scaling function at previous resolution. This is simply the M – Band extension of the two dimensional rule that we established in the previous section.

$$\psi_m(t) = \sum_n d_m(n)\phi(Mt - n) \quad \textbf{(4.16)}$$

We also have established that the scaling function must be orthogonal to each wavelet in the M – Band system of wavelets. This can be written as

$$\langle \psi_m(t), \phi(t-l) \rangle = \sum_n d_m(n) \langle \phi(Mt-n), \phi(t-l) \rangle \tag{4.17}$$

The dot product on the right hand side of (4.17) can be reduced using (4.3) and (4.5) to be

$$\langle \phi(Mt-n), \phi(t-l) \rangle = \frac{c(n-Ml)}{M} \tag{4.18}$$

allowing us to write (4.17) as

$$\langle \psi_m(t), \phi(t-l) \rangle = \sum_n d_m(n) \frac{c(n-Ml)}{M} \tag{4.19}$$

As stated above, the scaling function and each wavelet must be orthogonal, which implies that (4.19) must be identically equal to zero or

$$\sum_n d_m(n) \frac{c(n-Ml)}{M} = 0 \quad where\ m \in \{0,1 \ldots M-2\} \tag{4.20}$$

The same rules apply to the wavelet functions themselves, each wavelet should be orthogonal to every other wavelet in the M – Band system. Using the same methods that we used to arrive at (4.20), it can easily be shown that

$$\sum_n d_m(n) \frac{d_p(n-Ml)}{M} = 0 \quad where\ m, p \in \{0,1 \ldots M-2\}\ and\ m \neq p \tag{4.21}$$

The results in (4.19) and (4.21) can be written in the frequency domain as

$$\begin{aligned} &\sum_{q=0}^{M-1} \left[G^*_m\left(\omega + \frac{2\pi q}{M}\right) H\left(\omega + \frac{2\pi q}{M}\right) \right] = 0 \quad for\ each\ m \in \{0,1 \ldots M-2\} \\ &\sum_{q=0}^{M-1} \left[G^*_m\left(\omega + \frac{2\pi q}{M}\right) G_p\left(\omega + \frac{2\pi q}{M}\right) \right] = 0 \quad for\ each\ m, p \in \{0,1 \ldots M-2\}\ where\ m \neq p \end{aligned} \tag{4.22}$$

where we have used the formula in (4.8) to put the results in terms if the $H(\omega)$ and $G_m(\omega)$ filters. This development leads us to a compact result that can be written in a matrix form. Combining the results of (4.9), (4.15) and (4.22) we can write the following summation form shown in (4.23), which provides the properties of the scaling and wavelet filters that become crucial to our development. Define $P_0(\omega) \equiv H(\omega)$ and $P_i(\omega) \equiv G_{i-1}(\omega)$ for

$i \in \{1,2 \ldots M-1\}$, where H(ω) and $G_m(\omega)$ are the frequency responses of the discrete time filters in (4.8). The orthogonality conditions on the scaling filters and wavelet filters lead to (4.23)[46]

$$\sum_{m=0}^{M-1}\left[P_i^*\left(\omega+\frac{2\pi n}{M}\right)P_j\left(\omega+\frac{2\pi n}{M}\right)\right]=\delta_{i,j} \text{ for } i,j \in \{0,1 \ldots M-1\} \tag{4.23}$$

We can expand these results into the single matrix form shown in (4.24)

$$\begin{bmatrix} P_0(\omega) & P_0\left(\omega+\frac{2\pi}{M}\right) & \cdots & P_0\left(\omega+\frac{2\pi(M-1)}{M}\right) \\ P_1(\omega) & P_1\left(\omega+\frac{2\pi}{M}\right) & \cdots & P_1\left(\omega+\frac{2\pi(M-1)}{M}\right) \\ \vdots & \vdots & & \vdots \\ P_{M-1}(\omega) & P_{M-1}\left(\omega+\frac{2\pi}{M}\right) & \cdots & P_{M-1}\left(\omega+\frac{2\pi(M-1)}{M}\right) \end{bmatrix} \begin{bmatrix} P_0^*(\omega) & P_1^*(\omega) & \cdots & P_{M-1}^*(\omega) \\ P_0^*\left(\omega+\frac{2\pi}{M}\right) & P_1^*\left(\omega+\frac{2\pi}{M}\right) & \cdots & P_{M-1}^*\left(\omega+\frac{2\pi}{M}\right) \\ \vdots & \vdots & & \vdots \\ P_0^*\left(\omega+\frac{2\pi(M-1)}{M}\right) & P_1^*\left(\omega+\frac{2\pi(M-1)}{M}\right) & \cdots & P_{M-1}^*\left(\omega+\frac{2\pi(M-1)}{M}\right) \end{bmatrix} = \mathbf{I} \tag{4.24}$$

The commutative nature of (4.24) allows us to reverse the order of the above multiplication while maintaining the equations integrity. Performing this operation and expanding the results, generates the final governing filtering equations that we are interested in for the M – Band system.

$$\sum_{i=0}^{M-1}|P_i(\omega)|^2=1 \tag{4.25}$$

4.2 M – Band Bandlimited Orthogonal Wavelet Design

We start with the basic filter equation given in (4.26) where we have normalized (4.6) using the expression in (4.8).

$$\Phi(M\omega)=H(\omega)\Phi(\omega) \tag{4.26}$$

Assume Φ(ω) is bandlimited to a frequency ω_m, i.e. Φ(ω)=0 for $|\omega|>\omega_m$. Then, from (4.26), H(ω)=0 for the region between ω_m /M and π . Therefore,

$$\omega_m \leq M\pi \tag{4.27}$$

The Poisson Summation formula clearly indicates that the scaling function must have a bandwidth that is greater than π. We therefore rewrite the ω_m as

$$\omega_m = \pi + \alpha \tag{4.28}$$

Where α is some value greater than zero. From (4.26) we can also determine that

$$\begin{aligned} |\Phi(\omega)|^2 &= 1 \quad \text{for } 0 \leq \omega \leq \pi - \alpha \\ |\Phi(\omega)|^2 &= 0 \quad \text{for } \omega \geq \pi + \alpha \end{aligned} \tag{4.29}$$

We turn now to the filter that is defined by the scaling function in (4.26). The filter, H(ω), is discrete which forces the frequency response to be 2π periodic. For our purposes we will write this as

$$H(\omega) = H(\omega + 2\pi) = H^*(2\pi - \omega) \tag{4.30}$$

This, with the Poisson Summation formula, allows us to define regions of support for the filter itself. Using Figure 4.2 and Figure 4.3 as a visual aid and from (4.27),(4.28) and (4.30) we define,

$$\begin{aligned} H(\omega) &\neq 0 \quad \text{for } |\omega| \leq \frac{\pi + \alpha}{M} \\ H(\omega) &= 0 \quad \text{for } \frac{\pi + \alpha}{M} < \omega < \left[2\pi - \left(\frac{\pi + \alpha}{M}\right)\right] \end{aligned} \tag{4.31}$$

The periodic nature of H(ω) implies that we can write at the boundary of (4.31)

$$H\left(2\pi - \frac{\pi + \alpha}{M}\right) = H\left(\frac{(2M-1)\pi - \alpha}{M}\right) = 0 \tag{4.32}$$

We have attempted to depict the boundaries defined from the above conditions in Figure 4.2 below. The solid line shows the "ideal" filter H(ω) and the dotted line shows the shifted version of the filter by 2π. It should be recognized that this is simply a visual aid in deriving an expression for α. Clearly, as illustrated below, these two functions do not satisfy the rules dictated above. It is for this reason that we need to define the strict limitation on α that will satisfy our imposed restrictions.

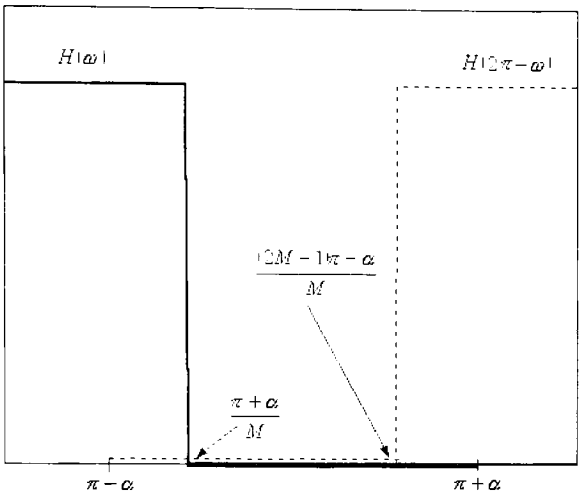

Figure 4.2 - Boundary conditions for the H(ω) filter frequency response. The extreme case is determined when the two band edges of H(ω) and H(2π−ω) coincide.

In the ideal (non-realizable) case α would be identically zero. This would place the transition band for H(ω) exactly at π/M and the defined stop band at π. This results situation as in Figure 4.3a.

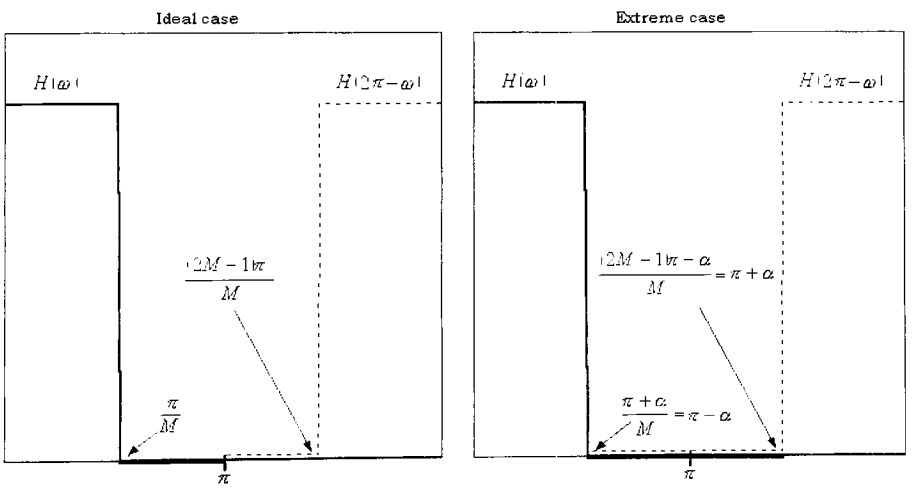

Figure 4.3a, 4.3b - Band extremes for the Meyer scaling function

The other boundary condition is when the stop band of the H(ω) filter lines up directly with the start of the transition band in the shifted version. This case provides us with the

limit that is necessary for the development of our α term and is shown in Figure 4.3b. The regions shaded in gray indicate the transition bands of our filters. As mentioned above these diagrams are merely tools for visualization and are not intended to depict the actual filters themselves. The specified regions illustrated are simply regions of support for the filters, this idea is that the filter is not equal to zero and less than one in the regions shown in gray. They are identically zero where the boundaries are zero and identically one in the enclosed white regions. From Figure 4.3b we can determine the limit on our α condition given the scaling function as

$$\alpha = \pi\left(\frac{M-1}{M+1}\right) \tag{4.33}$$

Our scaling function can be generated by choosing an α term in the range defined by

$$0 \le \alpha \le \pi\left(\frac{M-1}{M+1}\right) \tag{4.34}$$

To guarantee a valid scaling function the transition band must satisfy the Poisson Summation formula. We write this as

$$|\Phi(\omega)| = \begin{cases} 1 & 0 \le \omega < \pi - \alpha \\ \gamma(\omega) & \pi - \alpha \le \omega < \pi + \alpha \\ 0 & \text{otherwise} \end{cases} \tag{4.35}$$

The γ(ω) is a function that satisfies the transition band defined by the Poisson Summation formula

$$\gamma(\omega)^2 + \gamma(2\pi - \omega)^2 = 1 \tag{4.36}$$

If we let M=2 in (4.34) we see that it does indeed reduce to the expected value in the two – Band Meyer wavelet case which was the result of W.W. Jones in [4], however we will show in subsequent sections that tighter bounds on must be placed on (4.33) to generate an orthogonal bandlimited M – Band wavelet basis. Clearly the concept of the expression in (4.34) is closely

related to the roll-off factor of the square root raised cosine (SRRC) function, as shown in [31]. The exact relationship of the α parameter and the roll off factor is described in Appendix A. The function in (4.33) incorrectly implies that when we extend to the M – Band case, we increase the range under which the SRRC roll-off factor generates a valid scaling function.

4.3 The Composite Wavelet and Embedded Wavelets

In the previous section the magnitude of the scaling function for an orthogonal M – Band bandlimited wavelet system was clearly defined. We have yet to determine the wavelets themselves. To accomplish this the concept of a composite wavelet will be introduced. The squared magnitude of the composite wavelet will be defined as the following

$$|\Theta(\omega)|^2 = \sum_{m=0}^{M-2} |\Psi_m(\omega)|^2 \tag{4.37}$$

From our previous discussions on wavelet filters, we can establish that

$$G_m(\omega) = \frac{\Psi_m(M\omega)}{\Phi(\omega)} \tag{4.38}$$

This, in combination with (4.7) and (4.23) leads to the results in (4.39). A proof of this is provided in Appendix B.

$$|\Phi(\omega)|^2 = |\Phi(M\omega)|^2 + \sum_{m=0}^{M-2} |\Psi_m(M\omega)|^2 \tag{4.39}$$

The expression in (4.37) has been defined as the summation on the right hand side of (4.39), that is

$$|\Phi(\omega)|^2 = |\Phi(M\omega)|^2 + |\Theta(M\omega)|^2 \tag{4.40}$$

Similarly we can write (4.40) in terms of the filters

$$|H(\omega)|^2 + |\mathrm{A}(\omega)|^2 = 1 \tag{4.41}$$

where we have defined

$$\mathrm{A}(\omega) = \sum_{m=0}^{M-2} G_m(\omega) \tag{4.42}$$

If we now sum (4.38) over all valid m in our M – Band system and multiply both sides by the scaling function we acquire

$$\Phi(\omega)\sum_{m=0}^{M-2} G_m(\omega) = \sum_{m=0}^{M-2} \Psi_m(M\omega)$$

By substituting in the definitions that we have established for these sums we can compactly write this as

$$\Phi(\omega)A(\omega) = \Theta(M\omega) \tag{4.43}$$

This composite wavelet system is depicted graphically in Figure 4.4, the functions shown are not to scale and are drawn to depict the embedded nature of the functions. The actual shapes of the filters will be developed shortly, at which time will make reference to Figure 4.4 for the design. The idea is that there is a series of wavelets that are embedded within the composite wavelet such that the sum of their magnitudes results in the composite wavelet itself.

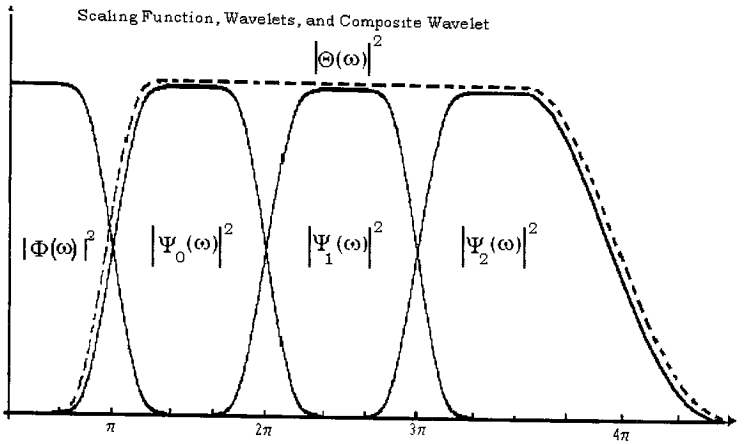

Figure 4.4 - Scaling function and composite wavelet (shown in dashes). The M-1 wavelets are embedded completely within the composite wavelet, such that the sum of the squares is the composite wavelet itself.

One may ask if the composite wavelet obeys the laws laid out by individual wavelet functions. In particular does the Poisson Summation formula apply to the composite wavelet, implying that integer translates of itself form an orthogonal basis. These results are explored in detail below.

The problem stated above is to determine *if* $\sum_p |\Theta(\omega + 2\pi k)|^2 = C$ where C is some constant value. If this holds true then the composite wavelet obeys the Poisson summation formula and θ(n) can therefore be considered to be a form of wavelet. Before we start the mathematical analysis it is important to get a nice visual representation of the problem that it is we are dealing with. Equation (4.40) relates the scaling function to the dilated scaling function and the dilated composite wavelet in the frequency domain, with which we can generate the plot found in Figure 4.5. The outer shape is the squared magnitude of the scaling function. Embedded within this function are two other

functions, one of which is the composite wavelet dilated by a factor of M and the other being the same scaling function also dilated by a factor of M. The sum of the magnitude squared of these two latter functions must be identically the scaling function itself. It can now be simply seen that the shape of the composite wavelets frequency response is immediately known when the scaling functions frequency response is known.

$$|\Theta(M\omega)|^2 = |\Phi(\omega)|^2 - |\Phi(M\omega)|^2 \tag{4.44}$$

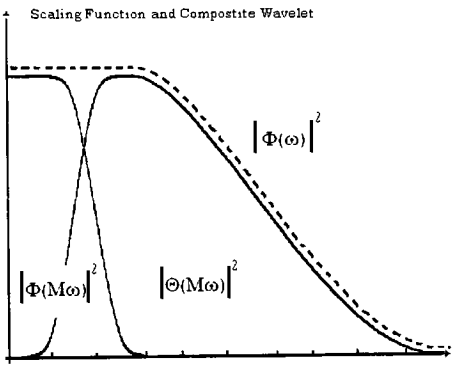

Figure 4.5- Scaling function and the M - Scale relationship with the composite wavelet.

Recall that $|\Phi(M\omega)|^2 + \sum_{p=0}^{M-2} |\Psi_p(M\omega)|^2 = |\Phi(\omega)|^2$ where we have defined the summation to be a function in Mω as

$$\sum_{p=0}^{M-2} |\Psi_p(M\omega)|^2 = |\Theta(M\omega)|^2 \tag{4.45}$$

The original stated problem can be reduced using (4.45)

$$\sum_{p}\left|\Theta(\omega+2\pi k)\right|^2 =$$

$$\sum_{k=0}^{M-1}\sum_{p=0}^{M-2}\left|\Psi_p(\omega+2\pi k)\right|^2 = \qquad \textbf{(4.46)}$$

$$\sum_{p=0}^{M-2}\sum_{k=0}^{M-1}\left|\Psi_p(\omega+2\pi k)\right|^2$$

Because we desire $\langle \psi_p(t), \psi_p(t-\tau)\rangle = \partial(\tau)$ we know that

$$\sum_{k=0}^{M-1}\left|\Psi_p(\omega+2\pi k)\right|^2 = 1 \qquad \textbf{(4.47)}$$

This implies that (4.46) simplifies to

$$\sum_{p=0}^{M-2} 1 = (M-1)$$

Therefore we can conclude that

$$\sum_{k=0}^{M-1}\left|\Theta(\omega+2\pi k)\right|^2 = (M-1) \qquad \textbf{(4.48)}$$

which implies that our composite wavelet is orthogonal to integer translates of itself. A similar approach to the filter A(ω) shows that it obeys the same governing rules as the filters H(ω) and $G_m(\omega)$ as in (4.24). Namely

$$\sum_{m=0}^{M-1}\left|A(\omega+\frac{2\pi k}{M})\right|^2 = (M-1) \qquad \textbf{(4.49)}$$

From equation (4.40), the composite wavelets shape can be determined once we have developed an expression for the associated scaling function. We have developed the rules for frequency domain relationships between the individual wavelets and the composite wavelet provided in (4.39) from which the form of each individual bandlimited wavelet can then be found. The 3db points for the composite wavelet in the 2 – Band case occur at both π and 2π. Extending this result to the M – Band case shows that the 3db points occur at π and Mπ (see Figure 4.6).

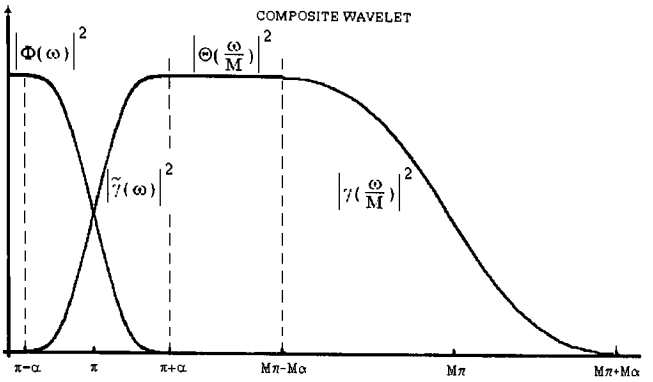

Figure 4.6 - The magnitude squared frequency response of the composite wavelet and its band edges.

As mentioned previously, this composite wavelet embeds the M-1 wavelet FT's. Looking at the structure of the composite wavelet yields clues as to how each individual wavelet's FT should reside within the form presented by the composite wavelet itself. If we take the starting band edge of the first embedded wavelet's FT to coincide with the starting band edge of the composite wavelet's FT and we take the stop band edge of the last embedded wavelet's FT to coincide with the stop band edge of the composite wavelet's FT, we have sufficient clues on how the embedded wavelet's FT should behave. As defined by the design there reside M-1 wavelet FTs within the composite wavelet. If we want to maintain uniform bandwidth we can write the average bandwidth of each element as

$$\overline{B}_{\psi} = \frac{M\pi - \pi}{(M-1)} = \pi \qquad \textbf{(4.50)}$$

This is consistent with the results of the Meyer wavelet and scaling function FTs. If one reexamines Figure 3.7, it clearly indicates that the 3dB point of the scaling FT and the wavelet FT intersect at the 3dB point located at π radians. We can therefore assume that the 3dB points of all wavelet FTs in the M – Band case should occur at intervals of $(m+1)\pi$ for m = 0,1...M-1 and proceed to verify the results with this assumption.

We have already illustrated that the scaling function essentially consists of three regions, a pass band, a transition band and a stop band. The pass band is identically equal to one in the range

$0 \le \omega < (\pi - \alpha)$. Similarly, the stop band is zero for the region where $\omega > \pi + \alpha$. The transition band has also been defined to exist such that (4.36) is completely satisfied.

$$\Phi(\omega) = \gamma(\omega) \text{ in the region } (\pi - \alpha) \le \omega < (\pi + \alpha) \tag{4.51}$$

The function that describes the transition band in the scaling function, γ(ω), must be such that

$$\gamma(\omega)^2 + \gamma(2\pi - \omega)^2 = 1$$

This equation is only important in the regions defined in (4.51). We can define a function $\tilde{\gamma}(\omega)$ that is the mirror image of γ(ω) in this region so that the above can be rewritten as

$$\gamma(\omega)^2 + \tilde{\gamma}(\omega)^2 = 1 \tag{4.52}$$

The composite wavelet is a band pass function that has five bands that of are interest to us, each of which can be determined from the shape of the scaling function. In Figure 4.6 we can see that the transition from stop band to pass band is defined as $\tilde{\gamma}(\omega)$. The composite wavelet maintains the shape of a dilated scaling function after this transition, as shown in equation (4.40). If we expand this function in (4.40) so that it is a function of ω not Mω then the shape of the function is defined not by Φ(ω) but $\Phi\left(\frac{\omega}{M}\right)$. This dilation causes the transition from pass band to stop band to be governed by the function $\gamma\left(\frac{\omega}{M}\right)$. We have already determined a function for γ(ω) in previous sections when we defined the scaling function, we therefore have a complete mathematical model for the magnitude of the frequency response for the composite wavelet as seen in Figure 4.6.

We can now use the above defined function, $\tilde{\gamma}(\omega)$, to describe the transition to pass band of the first embedded wavelet's FT. Similarly, we can use $\gamma\left(\frac{\omega}{M}\right)$ to describe the transition to stop band of the last embedded wavelet's FT. Using these details, along with the 3dB points defined by

(4.50), we can derive the remaining transition bands of each individual embedded wavelet's FT. As discussed above, the 3dB points of each wavelet's FT occur at $(m+1)\pi$ for m = 0,1...M-1 (see Figure 4.7). If for each embedded wavelet's FT we utilize a dilated transition to stop band function, $\gamma(\omega)$, dilated by the factor of (m+2) for m = 0,1...M-2 and center this function such that the 3dB point occurs at the designated values of $(m+2)\pi$, we find that on the last dilation function resides exactly on the stop band of the composite wavelet's FT. For instance in the M = 4 system shown in Figure 4.7, the transition to stop band function of the first embedded wavelet's FT is given by $\gamma\left(\frac{\omega}{2}\right)$, the second by $\gamma\left(\frac{\omega}{3}\right)$, and finally the third by $\gamma\left(\frac{\omega}{4}\right)$ which coincides with the transition to stop band of the M = 4 composite wavelet. The transition to pass bands can be generated using the same logic as described above, or simply with the knowledge that the Poisson summation formula must be satisfied. To satisfy this property, each transition to pass band must correctly overlap the transition to stop bands of its neighboring wavelet's FT such that the sum of the squares is identically one. The only way to properly satisfy this is if these bands are the mirror images of the overlapping transition to stop bands or, identically, dilated versions of $\tilde{\gamma}(\omega)$. Once again referencing Figure 4.7, the first transition to pass band in our M = 4 system would be $\tilde{\gamma}(\omega)$ and the final transition to pass band, occurring at $(M-1)\pi$, would be $\tilde{\gamma}\left(\frac{\omega}{3}\right)$.

Assuming that the transition band of each wavelet embedded within the composite wavelet occurs at multiples of the average wavelet bandwidth π, then to maintain the shape of the composite wavelet we must have for each wavelet

$$|\Psi_m(\omega)|^2 = \begin{cases} \left|\tilde{\gamma}\left(\frac{\omega}{m+1}\right)\right|^2 & for\ (m+1)(\pi-\alpha) \le \omega < (m+1)(\pi+\alpha) \\ 1 & for\ (m+1)(\pi+\alpha) \le \omega < (m+2)(\pi+\alpha) \\ \left|\gamma\left(\frac{\omega}{m+2}\right)\right|^2 & for\ (m+2)(\pi-\alpha) \le \omega < (m+2)(\pi+\alpha) \\ 0 & otherwise \end{cases} \tag{4.53}$$

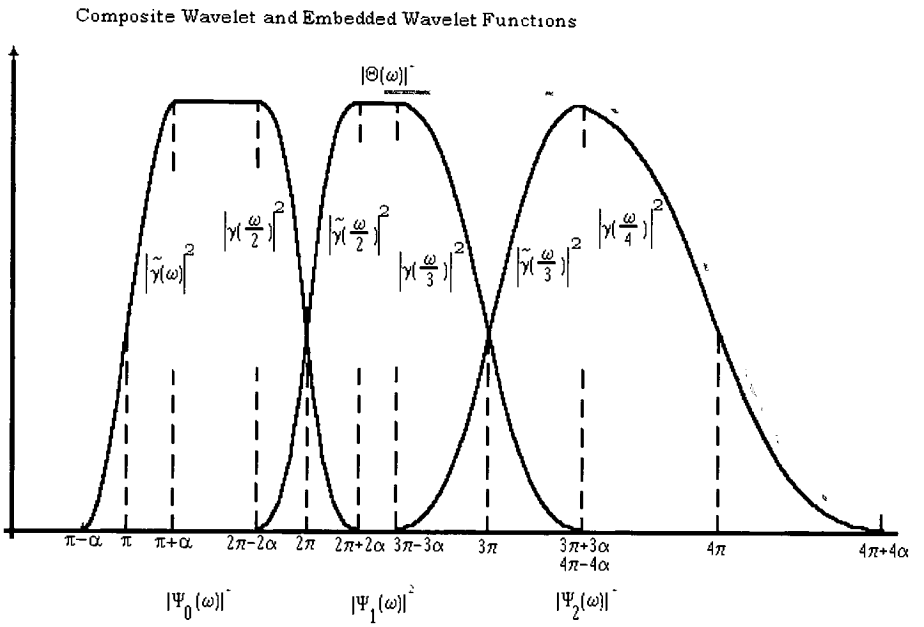

Figure 4.7 - The composite wavelet and the embedded wavelet functions. Notice the γ(ω) and $\tilde{\gamma}(\omega)$ as transition bands of each wavelet.

The design is such that for any overlapping transition band between two neighboring wavelets the following holds true

$$\gamma\left(\frac{\omega}{m}\right)^2 + \tilde{\gamma}\left(\frac{\omega}{m}\right)^2 = 1 \tag{4.54}$$

Previously, we defined α such that the scaling function and the composite wavelet correctly interact. There is an issue with this value that arises when dealing with individual wavelets. If we choose α to be exactly $\pi\frac{M-1}{M+1}$ then the transition to pass band of the last wavelet will extend past the transition to stop band of the first wavelet. This will create issues as all wavelets will

overlap one another, clearly violating the Poisson Summation that has been already determined. As we have indicated, we want the transition bands $\gamma(\omega)$ and $\tilde{\gamma}(\omega)$ to overlap without the interference from other wavelet filters. Essentially we require that only neighboring wavelet bands can overlap in the transition band. For this to hold true we need to examine the bounds on the last transition to pass band, (M-1), and the second to last transition to stop band (M-2). In the best case scenario these two bands can be neighboring points, we therefore write

$$(M-1)\pi-(M-1)\alpha \geq (M-2)\pi+(M-2)\alpha$$

Solving this equation for α, uniquely determines a new value of α that limits our choice for the original scaling function design.

$$\alpha \leq \frac{\pi}{2M-1} \tag{4.55}$$

The result in (4.55) provides our governing value for the wavelet design and supercedes the one presented in (4.33). Generating a scaling function, as we did in (4.35), using the α term given in (4.55) generates appropriate band limited orthogonal M – Band wavelets. It should be noted that in the two – Band case (M=2) the above equation reduces to the basic Meyer scaling function and boundary conditions. It is only coincidence that the results shown in (4.34) appear to work for M=2.

As the number of bands (M) in our design increases our restriction on α becomes tighter and tighter. This is due the fact that for larger number of bands we require obviously more filters. Because each filter widens as we move further from $\Psi_0(\omega)$ we have more opportunities for wavelet functions to overlap. If we pull the transition bands in we prevent them from overlapping and violating the M-Scale relation in (4.39). W.W. Jones' solution to this problem ended in the α term shown in (4.33). For this expression as M increases the α term becomes closer to π. This immediately dictates that the scaling function and wavelet tend to spread out in frequency

(resulting in a narrower time pulse) as the number of bands grows without bound. We have found that this is not the case but instead the α term has an inverse relationship to the number of filters in the system. In this case as M increases, α approaches zero, moving our scaling function closer to the ideal Shannon scaling function. This shows that as M increases our filters in the system move toward the uniform bandwidth π. It becomes clear at this point that the M – Band extension actually places further restrictions on our allowable choices for the SRRC pulse, indicating that the pulse can only be considered a valid wavelet in a tighter range of roll-off parameter as M increases.

4.4 Phase Response of the Scaling Function and Wavelets

For this development it is essential that we have already derived the appropriate expressions for the magnitudes of the M – Band wavelets and scaling function. Due to the non ideal nature of these filters, there are overlapping regions in the magnitude solution. Phase solutions for these functions that are relative to the scaling function, $H(\omega)$, can provide for the proper cancellation as needed for our system to satisfy the orthogonality criterion.

From the orthogonalitly of the scaling function and wavelet we can write

$$\sum_{k=-\infty}^{\infty} \Phi(\omega + 2\pi k)\Psi_0^*(\omega + 2\pi k) = 0$$
$$\sum_{k=-\infty}^{\infty} \Psi_i(\omega + 2\pi k)\Psi_j^*(\omega + 2\pi k) = 0 \ \textit{for } i, j \in \{0,1 \ldots M-2\} \textit{ where } i \neq j \tag{4.56}$$

We are also aware of the M scale relationship between of the scaling function and the wavelet as

$$\Phi(\omega)=P_0\left(\frac{\omega}{M}\right)\Phi\left(\frac{\omega}{M}\right) \quad and \quad \Psi_i(\omega)=P_{i+1}\left(\frac{\omega}{M}\right)\Phi\left(\frac{\omega}{M}\right) \; for \; i\in\{0,1\ldots M-2\} \tag{4.57}$$

If we substitute (4.57) back into (4.56) and reduce the expression with the knowledge that

$$\sum_{k=-\infty}^{\infty}\left|\Phi(\omega+2\pi k)\right|=1 \tag{4.58}$$

we arrive at the solution

$$\sum_{k=-\infty}^{\infty}P_{m-1}\left(\omega+\frac{2\pi k}{M}\right)P_m^*\left(\omega+\frac{2\pi k}{M}\right)=0 \quad for \; m\in\{1,2\cdots M-1\} \tag{4.59}$$

The bounds on (4.59) become critical in the phase solution development and it should be clearly noted that they extend across all integer k. We are only interested in the phase for the adjacent wavelets and scaling function due to the physical structure of the system. The filters are designed such that only these neighboring functions overlap. Non-adjacent wavelets immediately satisfy the orthogonal relationships due to the product always being identically zero, which is attributed to these filters non overlapping regions of support. We define a new variable, **q**, that indexes the overlapping regions as follows

$$q=\{0,1,2\ldots M-2\}$$

Figure 4.8 illustrates the first pair, $P_0(\omega)$ and $P_1(\omega)$, overlap where q=0. The second pair, q=1, would define the region where $P_1(\omega)$ and $P_2(\omega)$ overlap, and so on until the final pair $P_{M-2}(\omega)$ and $P_{M-1}(\omega)$ overlap . With q, we can develop an expression for the required shift to properly satisfy cancellation of these overlapping regions in (4.59). If we define a function z(q) as

$$z(q)=\begin{cases}\dfrac{M}{2(q+1)} & for \;\; 0\le q<\dfrac{M}{2}\\[2ex] \dfrac{M}{2M-2(q+1)} & for \;\; \dfrac{M}{2}\le q\le M-2\end{cases} \tag{4.60}$$

The resulting phase shift required to satisfy (4.59) becomes

$$\rho_q(\omega)=e^{-jz(q)\omega} \tag{4.61}$$

This results in the relationship between scaling function and wavelets as

$$P_m(\omega) = \rho_{m-1}(\omega) P_{m-1}^*\left(\omega + \frac{2\pi}{M}\right) for\ m \in \{1,2 \ldots M-1\} \quad \textbf{(4.62)}$$

A detailed development of the phase relationship can be found in Appendix C. Firstly it should be noted that the z(q) term does not always result in integer shifts. They are designed to rotate the shifts around the unit circle at the proper points so that cancellation properly occurs. Also each shift is with respect to the previous wavelet or scaling function. This implies that the total shift is accumulative, and with respect to the scaling function (which is defined with a phase of zero) the relative shifts continue to increase. We must now show that these phases do indeed satisfy the constraints placed on us in (4.59). To do this we will invoke a graphical argument and an example set of filters of M=4. It can be shown that this method will satisfy all filter orders, regardless if the order is even or odd. We present the methods for this particular case but the procedure remains the same for all higher orders as well. Firstly we illustrate the separation between the scaling function and the first wavelet in Figure 4.8 below.

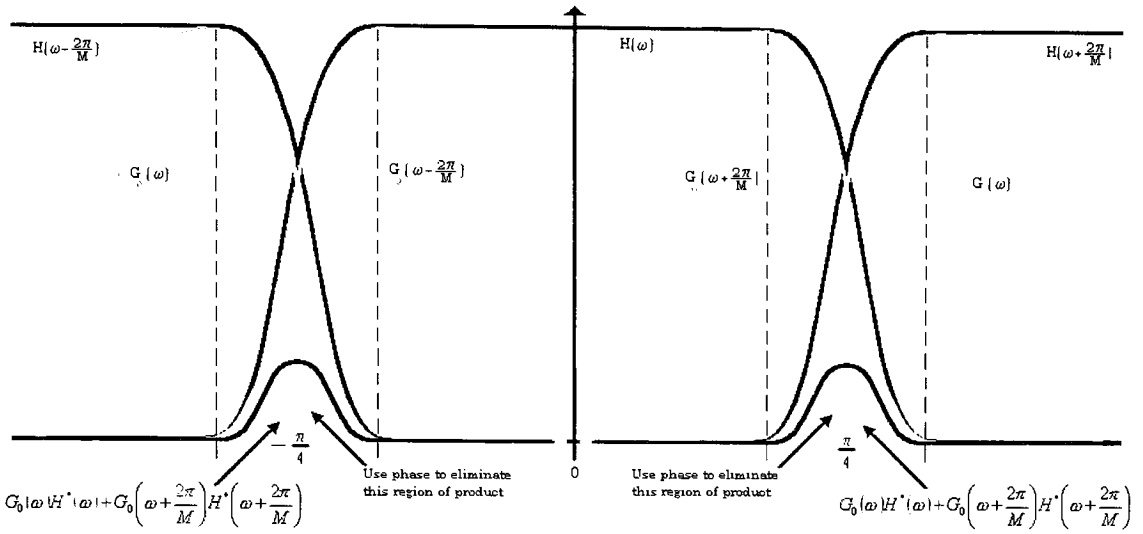

Figure 4.8 - Overlap of selected regions in the frequency domain (for M=4 as illustration). Phase will be used to eliminate the product "bumps" shown at the bottom.

For M=4 as we cycle through the summation formula in (4.59), it can be clearly seen that the bumps shift by an amount $\pi/2$. Therefore after each shift the next product will reside directly on top of the previous, this continues without bound. In order for the product to cancel out we must apply the proper phase to each frequency shifted version in the amount $e^{-j\pi}$. This implies that overlapping regions have opposite phase such their products sum to zero. This can be graphically seen in Figure 4.9, the y axis of the graph indicates the shift index that the summation is currently in and the x axis indicates the region where the product exists. The idea is to apply the proper phase to each shift so that the sums of all the shifts cancel out to be identically zero. At each shift index there is a corresponding phase that is applied to the wavelet so that this cancellation occurs, this value is given on the far left and is multiplied by the index before the shift occurs. The first row at the bottom of the chart is used to represent the overlap in Figure 4.8, the two additional blocks filled in that row are due to the periodic nature of the filters. Two shades of gray that are used in Figure 4.9 to represent the phase of the block in question,

the darker shade implies a zero phase and the lighter gray is a phase of π. Summing down the columns in our plot results in a zero value, due to the magnitudes being the same but the signal being π radians out of phase with the previous block. This zero value indicates that our developed phase relationship satisfies (4.59).

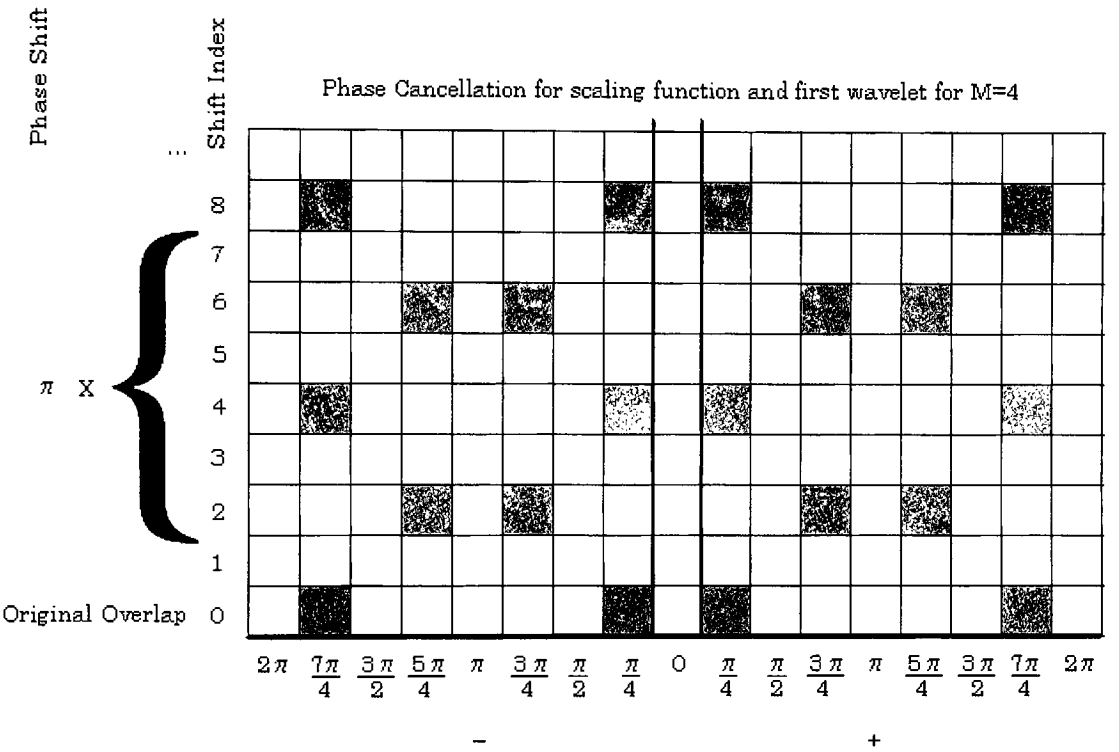

Figure 4.9 - The progressive phase cancellation of the scaling function and wavelet that occurs in (4.62)

The same procedure occurs for the remaining wavelets paying close attention to the fact that the overlapping regions in the wavelets are not located at π/4, but instead change as the filters progress. The number of phases applied also changes for the next wavelet pair, for proper cancellation we require 4 phases so that the overlap results in a sum of zero. We have employed 4 shades of gray to illustrate the for phases needed. In this case the phases are pair wise orthogonal. The last plot shows the phase relationship for the second

and final wavelet. This plot returns to the phase pattern of the scaling function and first wavelet but the starting location of the overlapping region differs. These locations, frequency shifts and appropriate phase shifts are all captured in the equations above.

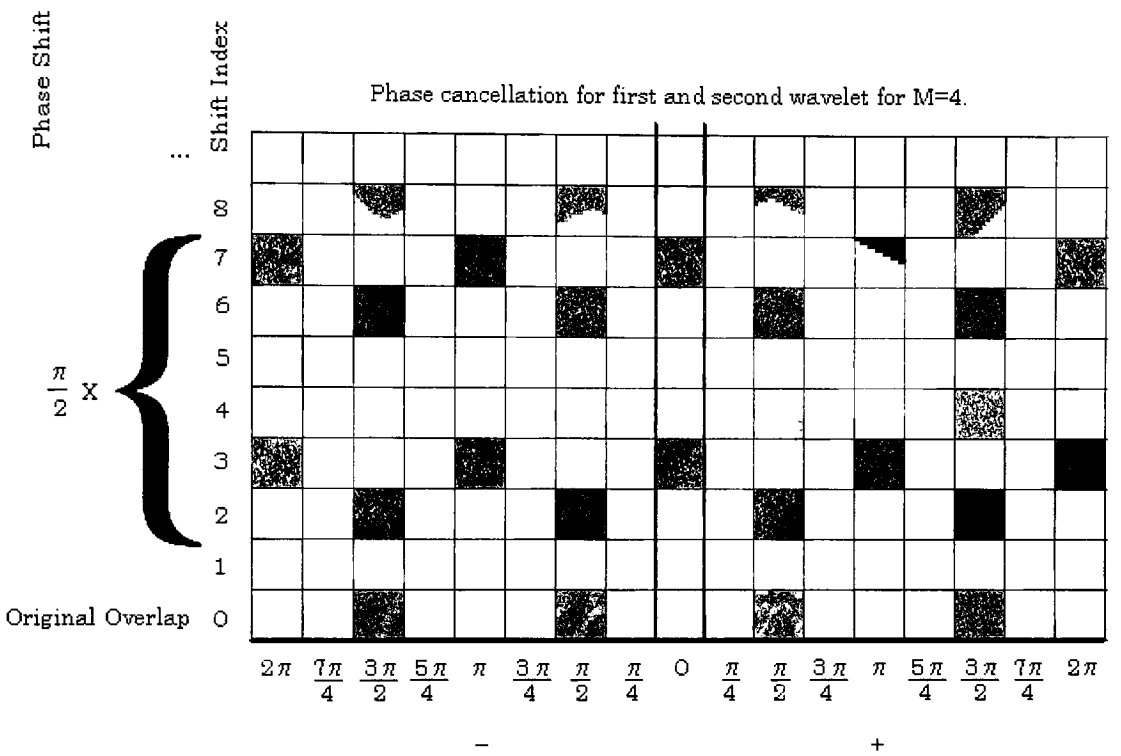

Figure 4.10 - The four phases required for cancellation in the first and second wavelet pair.

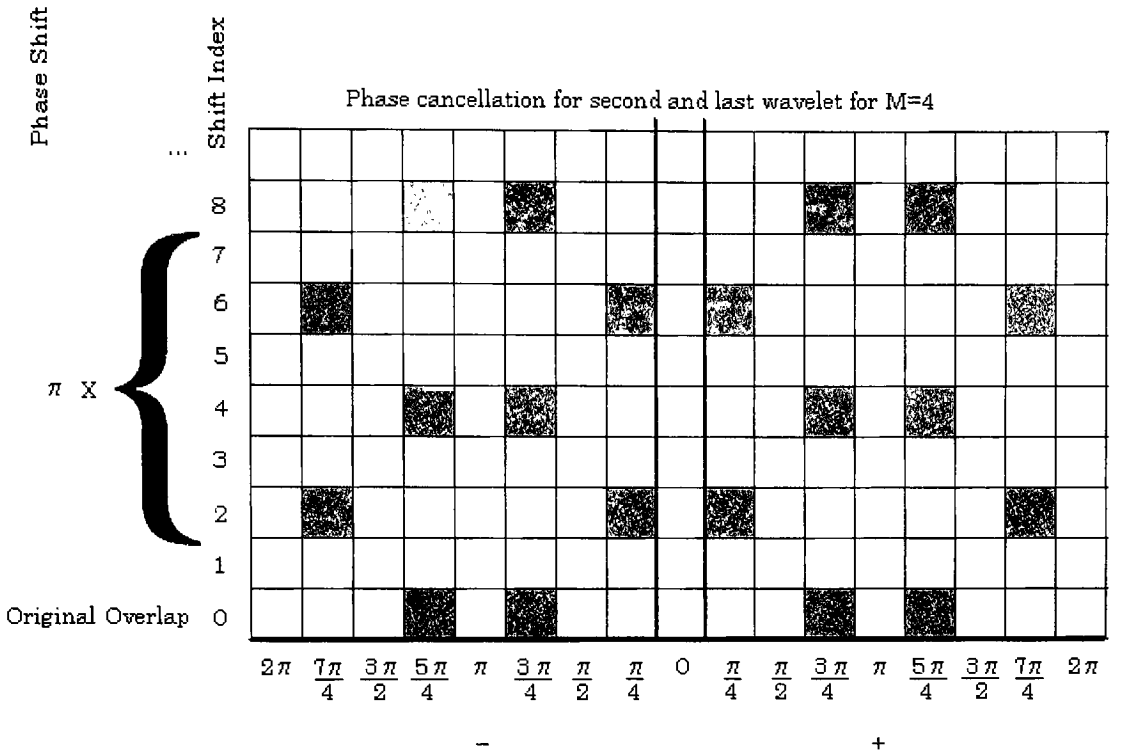

Figure 4.11- The four phases required for cancellation in the second and final wavelet pair.

Chapter 5

Examples

In this section we present several cases under which our above developed theory applies. We start be generating an orthogonal bandlimited M – Band wavelet construction with M=4. We will assume a best case α for an extreme case. In this set we will apply the complete construction technique for the scaling function composite wavelet, the three embedded wavelets and associated filters. We will then refine our results by generating a second filter bank by using a tighter α of $\pi/40$. This set will then be applied to a signal for demonstration of the decomposition and construction process. We will illustrate the error of the reconstruction process to show that given our chosen number of filter taps the error is minimal due to the FIR approximation. As a final example we will illustrate the design for a M=7 filter bank.

We start with the knowledge that our system is broken into four separate bands. Referring to (4.55) we see that

$$\alpha = \frac{\pi}{(2 \cdot 4 - 1)} = \frac{\pi}{7} \tag{5.1}$$

We use this fact to construct our $\gamma(\omega)$ function for the scaling function. We have shown that any function that satisfies (4.52) will generate an acceptable M – Band system. For this case we have chosen $\gamma(\omega)$ to take on a section of the cosine function. We have chosen

this particular function for $\gamma(\omega)$ but, as stated, the design is not restricted to this shape. There may be situations where this shape could be tailored to suit the transforms application.

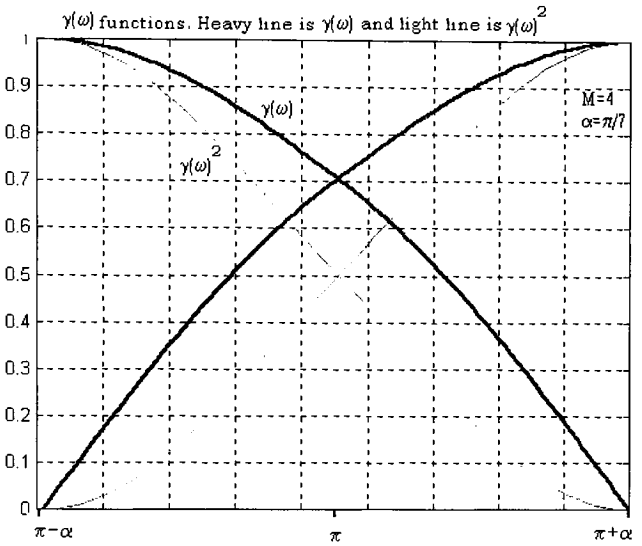

Figure 5.1 – $\gamma(\omega)$ and $\tilde{\gamma}(\omega)$ for M=4 and $\alpha=\pi/7$

Defining this function, $\gamma(\omega)$, is crucial to the remainder of the wavelet development, for as we have seen, this function defines the remainder of the filter bank development. From this shape and our knowledge of the bounds on the scaling function, we can now readily sketch out the remainder of $\Phi(\omega)$. Notice that the transition band is the heavy line in Figure 5.1.

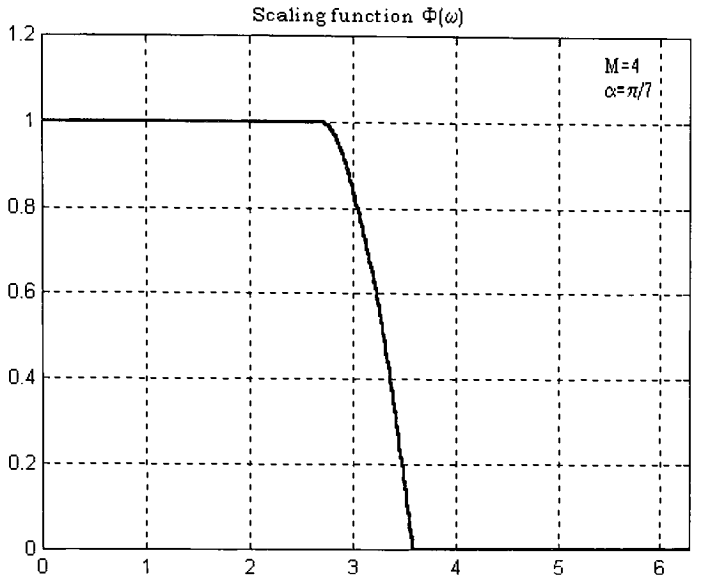

Figure 5.2- M=4 Meyer scaling function, Φ(ω).

The M scale relationship that we developed in (4.44) allows to quickly develop the composite wavelet which will contain the embedded wavelets of our M – Band system.

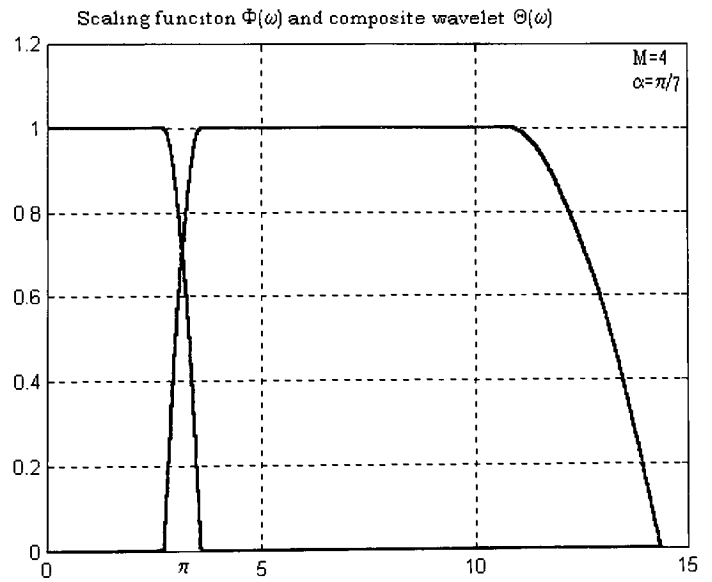

Figure 5.3 - Scaling function and associated composite wavelet for Meyer 4 band filter bank. There are 3 embedded wavelets within the composite wavelet shown.

The rising edge of the composite wavelet is defined by the $\tilde{\gamma}(\omega)$ shown in Figure 5.1.

We have also already established that the shape of the composite wavelet is derived from the shape of the dilated scaling function. This implies that the falling edge of the filter (in our M = 4 case) is governed by the shape given by $\gamma\left(\frac{\omega}{4}\right)$. As previously mentioned there are three wavelets embedded in the composite wavelet design. These three functions are also uniquely described by the $\gamma(\omega)$ that we arrived at. The midpoint of each transition occurs at $(m+1)\pi$ where m is the wavelet function index $\{0,1,2\}$. Each successive wavelet dilates the $\gamma(\omega)$ function by another factor of M. The passband region of each wavelet is identically one and the stop band identically zero. From this we can arrive at all three embedded wavelets, which is clearly illustrated in Figure 5.4.

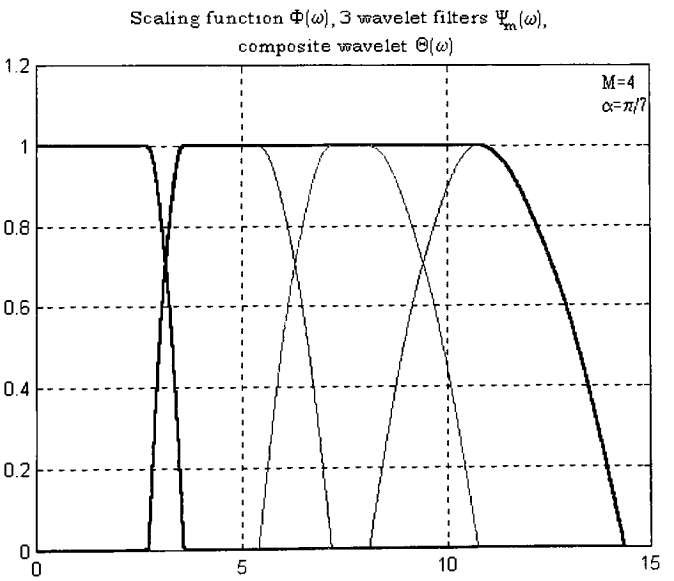

Figure 5.4 - Scaling function and wavelets embedded within the composite wavelet for M=4.

The overlap of the functions in Figure 5.4 is quite severe, this is due to our choice of α. From Figure 5.4 we can see that the embedded wavelets frequency response does indeed sum to the composite wavelets. In addition it can also be seen from this figure that the

sum of the squares of all wavelet frequency responses and scaling function frequency response results in the dilated scaling function, this is what we would expect from the M scale relationship. Figure 5.5 illustrates the scaling function and wavelets in the time domain, notice the signals do indeed oscillate outward toward infinity but the majority of the energy is contained within a narrow range around the origin. It can be shown that these signals are all orthogonal to one another and that their energies meet the requirements set up in earlier sections of this document. The scaling function and the corresponding wavelets are also smooth and closely resemble the dyadic Meyer representation. One point that we should notice in this example is the duration under which the signal energy is spread. We will find that as we increase our α term the energy will be supported less compactly than in the case below. This implies that if we are modeling these functions with a finite number of taps we will need to utilize more coefficients for wavelets with smaller α terms. This is presented in Figure 5.9 clearly.

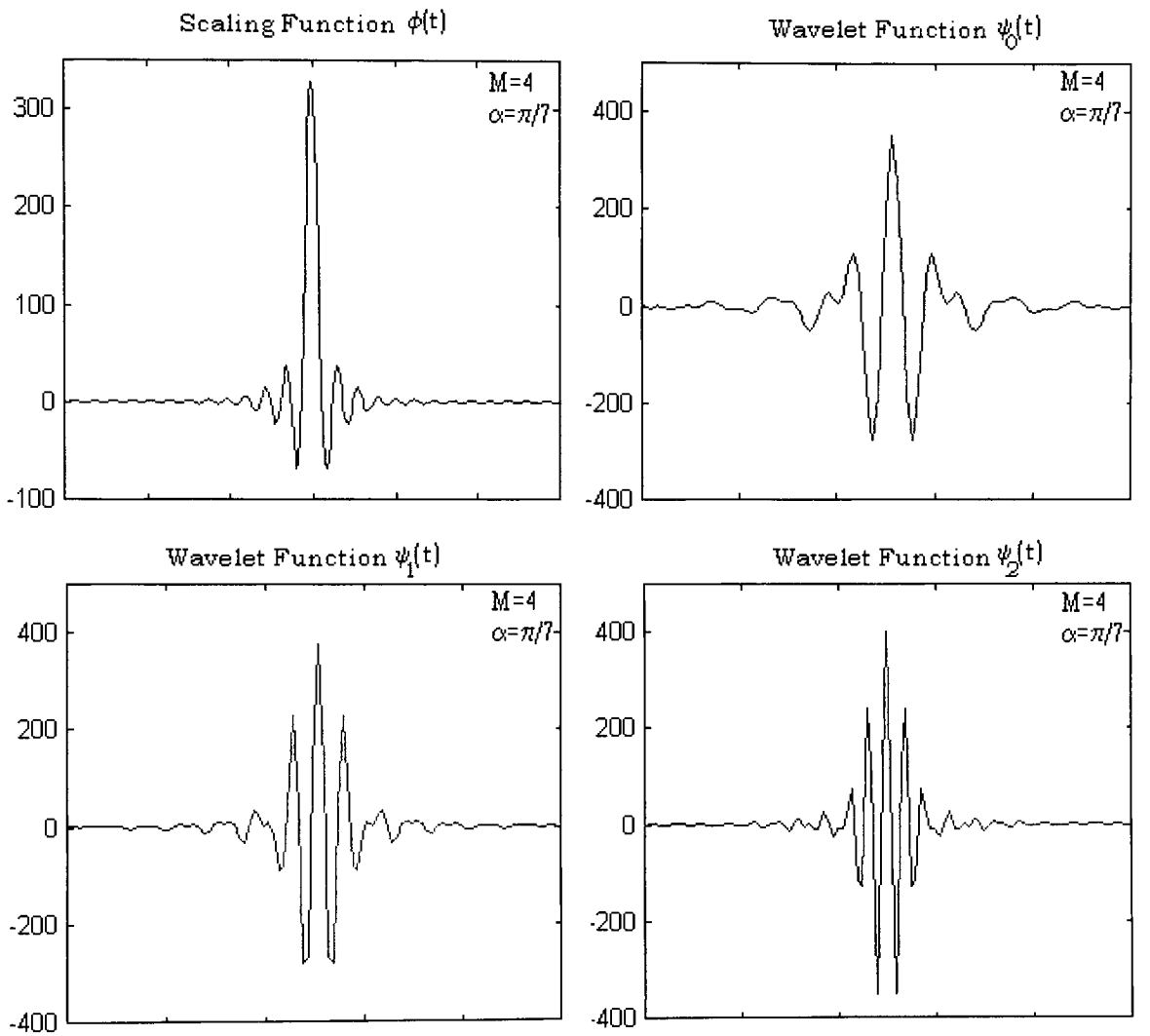

Figure 5.5 - Time domain representation of the Meyer wavelets as scaling function for M=4.

The corresponding filters for these functions are generated using equations (4.26) and (4.38). These are depicted in Figure 5.6. The shown filters are generated by truncating the number of samples of the time domain representation using a boxcar window. This approximation is not ideal and accounts for any loss in the pass band during implementation. They are clearly band limited filters which closely resemble their corresponding scaling functions and wavelet. The filters shown are $H(\omega)$, $G_0(\omega)$, $G_1(\omega)$ and $G_2(\omega)$ respectively. As mentioned above the overlap is significant but can be reduced by choosing a smaller α term. The filter taps can be derived directly from the Fourier transform of the filters in Figure 5.1 with phase applies in the frequency domain as given by expression (4.62).

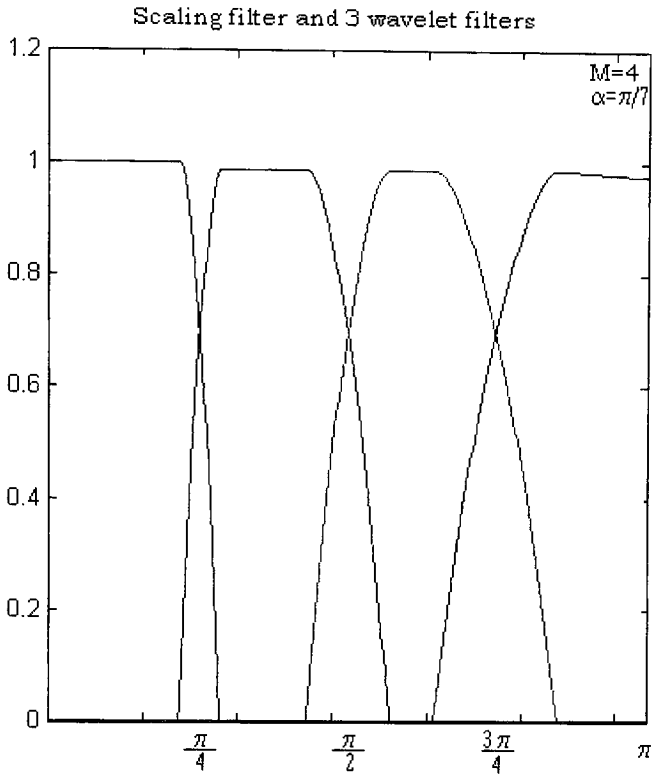

Figure 5.6 - Sample filters for M=4 and $\alpha=\pi/7$.

The example given above was the largest value of α that could be used without resulting in overlap between the non-neighboring filters. The filters provide a nice illustration of the development process but generate bands that have a large amount of frequency redundancy. This redundancy causes the filters not to have nice bounds under which the signal is decomposed, but instead we get large portions of the decomposed signal replicated across adjacent bands. Clearly this is not an issue as the filters themselves are designed as a perfect reconstruction filter bank and handle this redundancy. This overlap can never be completely eliminated but can be reduced by creating filters with tighter α term. One side effect of tightening this parameter is that the resulting filters require a larger number of taps to properly contain the majority of the filter energy when

approximation methods are being used. The example given below will illustrate the results of a M=4 filter with α set to $\pi/40$. The development of these functions is the same as the method utilized above, with the only difference being in the value that was chosen for α. Figure 5.7 illustrates the resulting scaling function and wavelet FTs and Figure 5.8 show the corresponding filters.

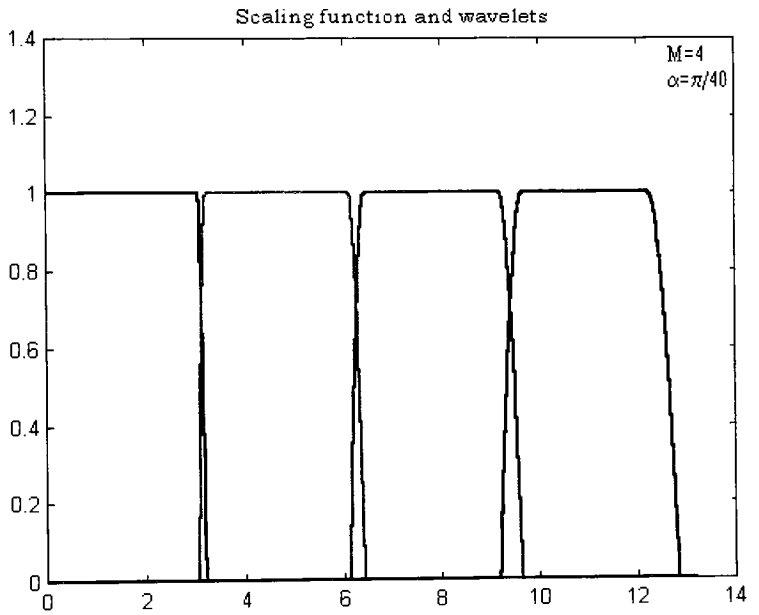

Figure 5.7 - Scaling function and wavelets for the M=4 case. Here we have let $\alpha=\pi/40$

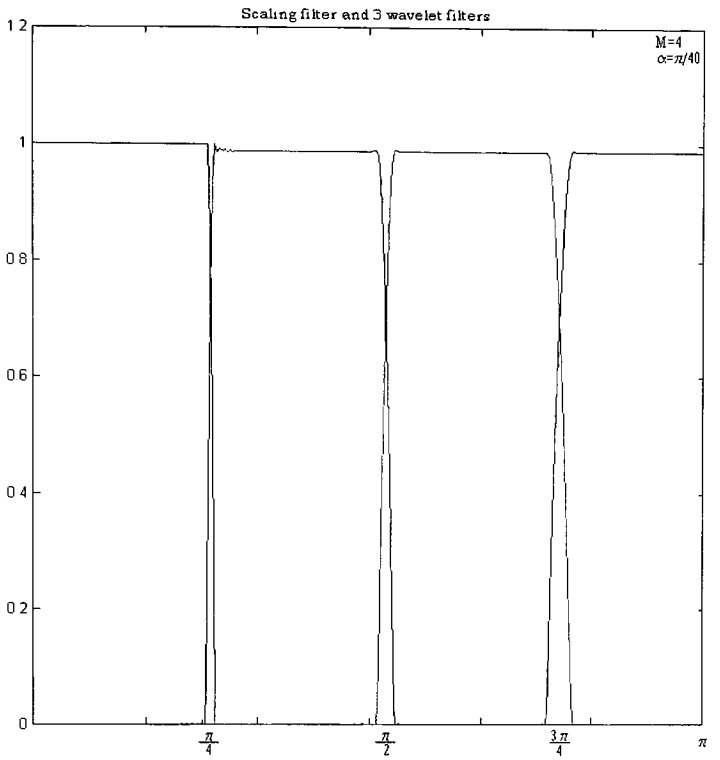

Figure 5.8 - Corresponding filters for $H(\omega)$ and $G_m(\omega)$. Notice the much tighter bounds on these filters than in the previous example.

Figure 5.9 shows the resulting scaling function and wavelets require more taps due to the fact that they have energy spread further out in time. These functions can be contrasted against the $\alpha=\pi/7$ case in Figure 5.5 to see the effect of the tightening of this α term. We utilize these filters generated to decompose and recompose the arbitrary input signal in Figure 5.10 composed of 5 sine waves of various frequencies and phases spread over the allotted frequency band (Fs = 8kHz).

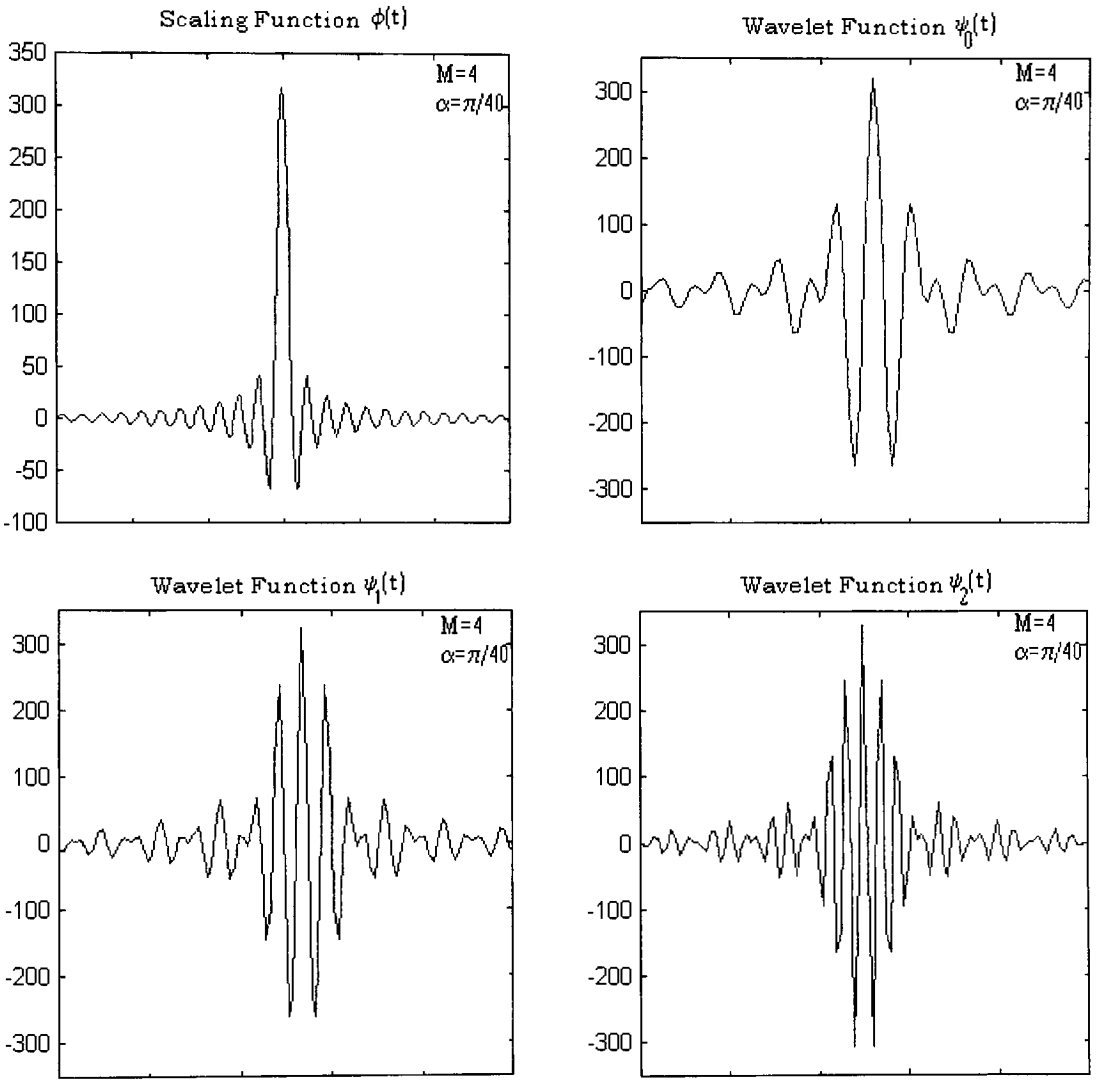

Figure 5.9 - M-Band scaling functions and wavelets in the time domain. Here M=4 and $\alpha=\pi/40$. Notice the spread of the signal in reference to the M=4 case.

The input signal is passed through the scaling filter and each wavelet filter then decimated by a factor of M to provide the results in Figure 5.11. This represents each output from the four filter bands, low pass, two band pass, and high pass respectively. The synthesis filters in the are simply the flipped versions of the analysis filters. We can then pass the up-sampled results of each band through these synthesis filters and by summing them together obtain the original sequence, presumably with no error. There is, however, a small amount of error due to the FIR approximation methods that we used. Our filters utilized a 100 taps with an α of $\pi/40$. The resulting recomposed signal is shown in Figure 5.12 with the error signal depicted in Figure 5.13. If the amount of error is determined to be unacceptable one can implement an IIR design different from the FIR approximation that we have used. We have also used a boxcar window to truncate our filter taps, it may be better to utilize a smoother windowing function like the Hamming or Blackman window. Our particular example resulted in a mean squared error (MSE) of $8.9347E^{-4}$ and a signal to noise ratio (SNR) of 68.9dB.

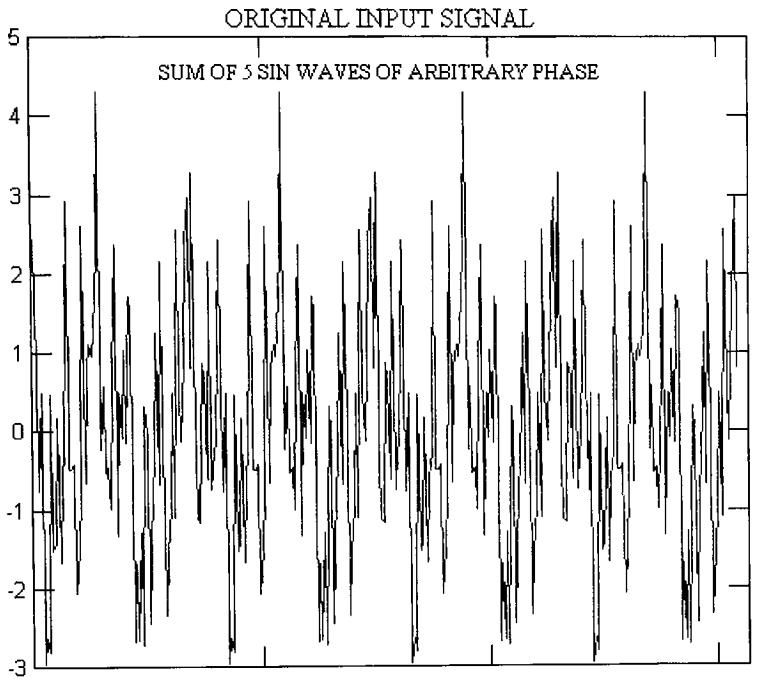

Figure 5.10 - Original input signal composed of 5 sine waves of arbitrary phase

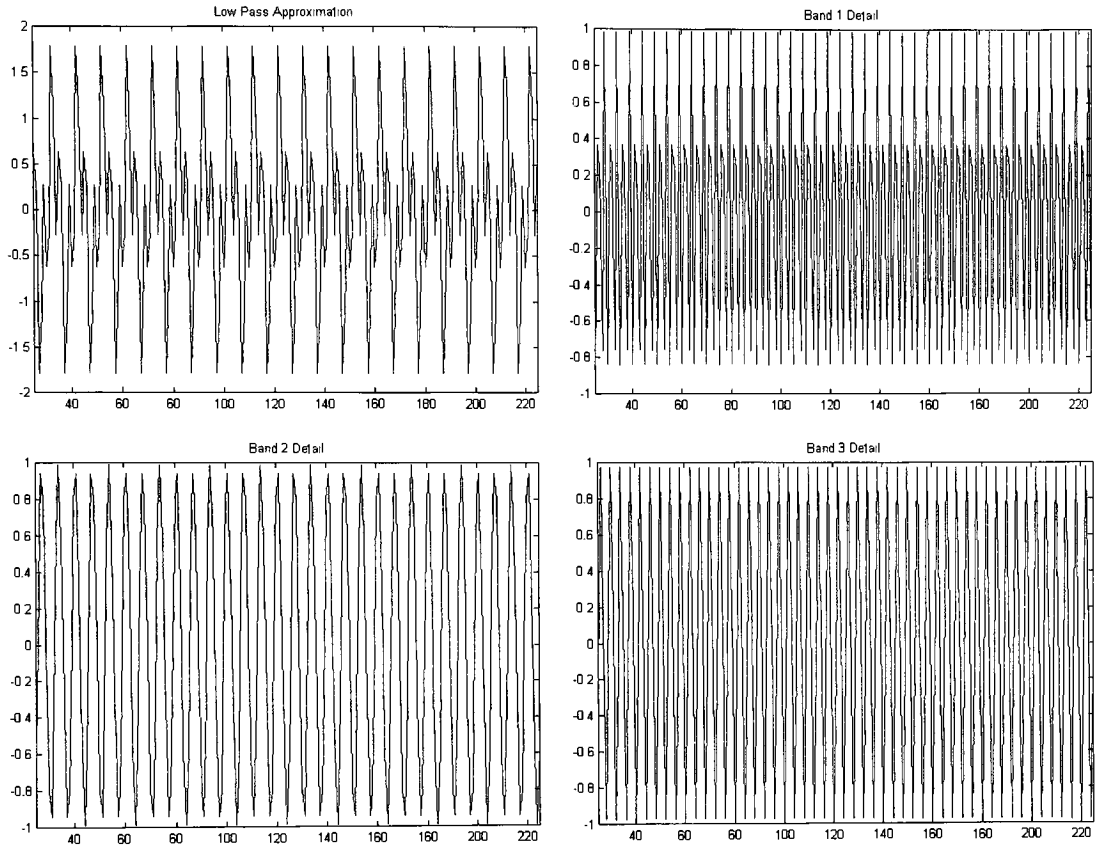

Figure 5.11 - Low pass approximation and three band details for the orthogonal M=4, $\alpha=\pi/40$, bandlimited wavelet decomposition. The results are the filtered and decimated signal.

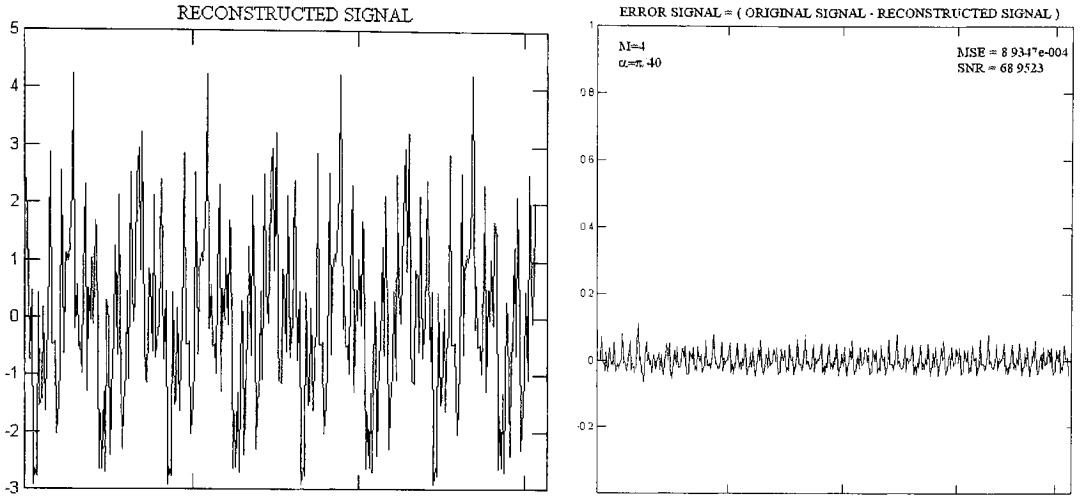

Figure 5.12, 5.13- The reconstructed signal and the error signal. The error in this system is completely attributed to the approximation of the filters by using a finite number of filter taps. This is especially apparent in systems with small a terms.

As a final example we will provide the results of a seven – Band wavelet system. The α term used here is again maximum value. In this case our maximum α term is sufficiently small in its own regard to require a large number of taps to approximate each wavelet and scaling filter. For M=7 we have an α of $\pi/13$. We show the scaling function, the composite wavelet and the corresponding 6 band limited wavelets in Figure 5.14

This system generates a set of 7 filters that will be used to decompose the input signal. In this case there is a single low pass approximation filter, a single high pass detail filter and 5 band pass detail filters. As in the four – Band case, these filters can be used to break the input into 7 separate bands for analysis and reconstruction. The importance in the choice of the α term is more apparent in this system as the overlap is spread throughout all the filters in this system. Again all 7 filters are strictly band limited

resulting in wavelets and a scaling function that extends across all t. The importance of this example is that it illustrates a design where M is odd valued. There is no limitation on the value placed on M which increases the flexibility of the filter design.

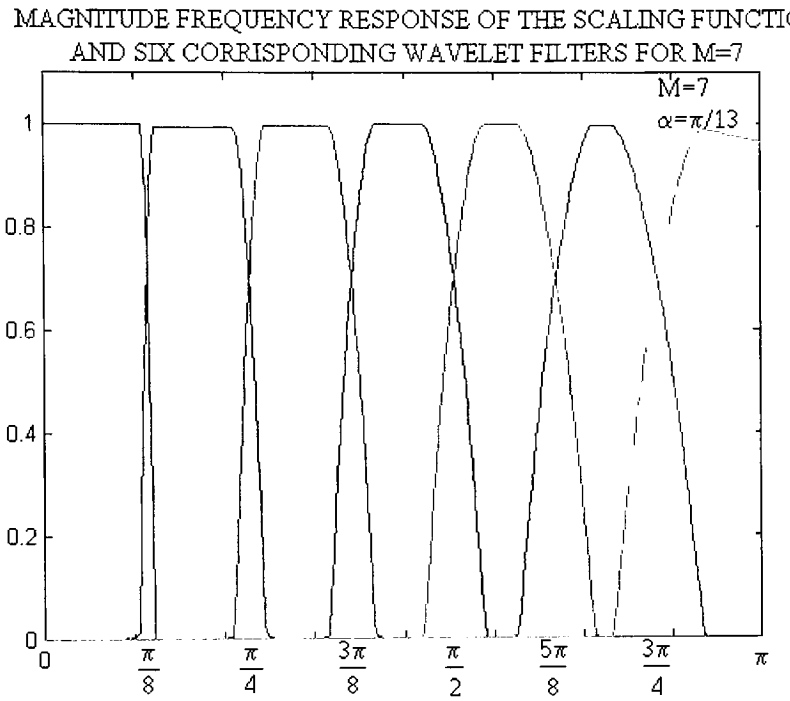

Figure 5.14 - Magnitude response of a M=7 wavelet filter bank. The α was chosen to be the extreme value π/13, the largest allowed term for this design.

Chapter 6

Conclusion

Wavelets have been shown to be an effective method of signal analysis. Their influence has spread to a multitude of signal processing applications. The link between the wavelet transform and filter banks opened up entire new theories and applications that have proven to be highly efficient and practical in application. From the earliest papers by Meyer and Mallat to the current papers of Vaidyanathan, Nguyen, and Vetterli, wavelets have grown into a mature field of the engineering sciences. In this thesis we examined one particular group of wavelets, a M – Band orthogonal bandlimited wavelet and scaling function, and applied the theory to generate a set of wavelet functions and filters. Of particular interest is the α term that provides a mathematical constraint on how rapidly the scaling function must transition from pass band to stop band. This term as discussed by other authors [4] in particular needed to be modified to properly support the neighboring wavelets. It was shown that without the correct term, non-adjacent wavelets could overlap which would violate the governing Poisson Summation formula. The design of these band limited wavelets is governed by determining a function, $\gamma(\omega)$, that satisfies a squared sum relationship. With this function determined, the scaling function and all subsequent wavelets can immediately be derived. Each wavelet and scaling function is band limited and results in an IIR filter. We further showed that a phase shift

is required between each successive wavelet to provide us with a solution to the orthogonality issues that are encountered in the wavelet design. The general design provides only a solution for the magnitude response of the filters, as described by the Poisson Summation formula. Separate steps are required to apply the proper phase shift of the filter so that perfect reconstruct is possible. In the process of developing the specific theory we also covered a general M – Band filter and wavelet theory.

Many implementations of M – Band wavelets have been designed in previous works by Vaidyanathan, Nguyen, Vetterli and others. Typically these filters are FIR filters with nice linear PR-QMF properties. One advantage that our design offers is in the smoothness of the band limited wavelet. This smoothness factor is particularly useful in image processing systems where the transitions tend to be hard edges. Our wavelet design offers an orthogonal band limited M – Band wavelet solution with nice filtering characteristics. The disadvantage to this approach is clearly in implementation. Utilizing an IIR filter can prove to be a difficult task, although computationally more efficient. We took the approach to model the scaling filter and wavelet filter with an FIR filter. This resulted in us having to utilize a large number of taps (100) to generate the filter response that we desired. The filters were used to analyze and reconstruct an arbitrary input signal consisting of 5 sine waves with random phase. The resulting decomposition and reconstruction resulted in a signal with a mean squared error (MSE) of $8.9347E^{-4}$ and a signal to noise ratio (SNR) of 68.9dB.

The design offers flexibility in the choice of the number bands, M, in the bank. In particular there is no restriction on whether the value is even or odd. This allows designs

suited to any number of required bands. We previously discussed to close simpliarity of the scaling function to the SRRC pulse. This relationship suggests a close relationship of these waveforms to communications. As W.W. Jones has pointed out in [4], these wavelets are ideally suited for waveforms in multi carrier modulation, their orthogonal and perfect reconstruction qualities provide for ideal non interfering waveform in this technique. The scaling function and each wavelet can be used as orthogonal waveforms to shape a data source via a PN chip sequence in a spread spectrum communication system. The M – Band nature of the filter bank allows for a uniform distribution of bandwidth, optimally distributing the information source across the allocated channel.

Also as a result of the theory developed in this thesis, steps have recently been taken to generate a model for an analogue voice scrambling technique to be embedded in a commercial high frequency radio. This wavelet analogue voice security (WAVS) feature is currently under investigation as next generation scrambling solution to analogue voice. Current methods employ a Fourier transform method to separate an input signal into frequency bands prior to scrambling. The filters of the current analogue voice security (AVS) are being replaced with wavelets as described above. It is believed that the result will be a higher fidelity, higher security scrambling technique using approximately the same number of MIPS as the previous generation AVS. In addition several recent papers have explored the intricacies of the Meyer wavelet, it is believed that the approaches and developments in this thesis can be applied to the results of mentioned papers as well.

Appendix A

The Relationship of the α Parameter to the Roll off Factor in the Square Root Raised Cosine (SRRC) pulse

As indicated in previous sections the α parameter that is used to describe the transition from start band to stop band of the scaling function is closely related to the roll off factor of the square root raised cosine pulse (SRRC). In the SRRC this roll off parameter is used to define the shape of the SRRC pulse as defined below

$$\hat{X}_{rc}(\omega)=\begin{cases}1 & for\ \ 0\le|\omega|\le\pi(1-\beta)\\ \frac{1}{2}\left[1+\cos\left(\frac{1}{2\beta}\left(|\omega|-\pi(1-\beta)\right)\right)\right] & for\ \pi(1-\beta)\le|\omega|\le\pi(1+\beta)\\ 0 & for\ \ |\omega|\ge\pi(1+\beta)\end{cases} \qquad \textbf{(A.1)}$$

where

$$0\le\beta\le1 \qquad \textbf{(A.2)}$$

If we return to (4.35) where we have defined the scaling function for our M – Band system we can see that the α parameter also defines the regions where the transition occurs from pass band to stop band. The relationship between the α parameter and the roll off parameter β can be determined by examining the behavior of these parameters at the bounds of the function. Namely from (4.35) and (A.1),

$$(\pi+\alpha)=\pi(1+\beta) \tag{A.3}$$

Solving for the β parameter in terms of α gives the simple relationship of

$$\beta=\frac{\pi}{\alpha} \tag{A.4}$$

Although $0\le\beta\le 1$ is a valid range for the SRRC pulse we have imposed tighter restrictions on α that will limit the valid available choices of roll off factor. In particular from (4.55) we have

$$0\le\beta\le\frac{1}{\pi(2M-1)} \tag{A.5}$$

Careful notice should be made of β's dependency on M, the number of bands in the filter bank. As we increase the number of bands we further restrict our available choices of SRRC pulses as valid scaling functions. Compiling these results together into (A.1) we can now determine an expression for valid a scaling function for any given M as

$$|\Phi(\omega)|=\begin{cases}1 & for\ \ 0\le|\omega|\le(\pi-\alpha)\\ \frac{1}{2}\left[1+\cos\left(\frac{\pi}{2\alpha}\left(|\omega|-(\pi-\alpha)\right)\right)\right] & for\ (\pi-\alpha)\le|\omega|\le(\pi+\alpha)\\ 0 & for\ \ |\omega|\ge(\pi+\alpha)\end{cases} \tag{A.6}$$

where α is given as in (4.55).

Appendix B

Definition of the Composite Wavelet

Because a matrix and its inverse are commute, we can reverse the order of (4.24) without compromising the integrity of the formulation. This allows us to reconstruct the matrix as

$$\begin{bmatrix} P_0^*(\omega) & P_1^*(\omega) & \cdots & P_{M-1}^*(\omega) \\ P_0^*\left(\omega+\frac{2\pi}{M}\right) & P_1^*\left(\omega+\frac{2\pi}{M}\right) & \cdots & P_{M-1}^*\left(\omega+\frac{2\pi}{M}\right) \\ \vdots & \vdots & & \vdots \\ P_0^*\left(\omega+\frac{2\pi(M-1)}{M}\right) & P_1^*\left(\omega+\frac{2\pi(M-1)}{M}\right) & \cdots & P_{M-1}^*\left(\omega+\frac{2\pi(M-1)}{M}\right) \end{bmatrix} \begin{bmatrix} P_0(\omega) & P_0\left(\omega+\frac{2\pi}{M}\right) & \cdots & P_0\left(\omega+\frac{2\pi(M-1)}{M}\right) \\ P_1(\omega) & P_1\left(\omega+\frac{2\pi}{M}\right) & \cdots & P_1\left(\omega+\frac{2\pi(M-1)}{M}\right) \\ \vdots & \vdots & & \vdots \\ P_{M-1}(\omega) & P_{M-1}\left(\omega+\frac{2\pi}{M}\right) & \cdots & P_{M-1}\left(\omega+\frac{2\pi(M-1)}{M}\right) \end{bmatrix} = \mathbf{I} \qquad \textbf{(B.1)}$$

Expanding the first row of the matrix multiplication yields the summation

$$\sum_{i=0}^{M-1} |P_i(\omega)|^2 = 1 \qquad \textbf{(B.2)}$$

Which can be rewritten as

$$|P_0(\omega)|^2 + \sum_{i=1}^{M-1} |P_i(\omega)|^2 = 1 \qquad \textbf{(B.3)}$$

Recall that we have redefined the filters $H(\omega)$ and $G_m(\omega)$ to be elements of the **P** matrix. With substitution we therefore have

$$|H(\omega)|^2 + \sum_{m=0}^{M-2} |G_m(\omega)|^2 = 1 \tag{B.4}$$

The M scale relationships in (4.6) and (4.7) are reiterated here for reference

$$M\Phi(M\omega) = C(\omega)\Phi(\omega) \tag{B.5}$$

$$M\Psi_m(M\omega) = D_m(\omega)\Phi(\omega), \; m = 0,1 \ldots M-2 \tag{B.6}$$

In addition recall that we have defined $H(\omega) = \frac{C(\omega)}{M}$ and $G_m(\omega) = \frac{D_m(\omega)}{M}$. This allows us to reduce (B.5) and (B.6) to

$$H(\omega) = \frac{\Phi(M\omega)}{\Phi(\omega)} \tag{B.7}$$

$$G_m(\omega) = \frac{\Psi_m(M\omega)}{\Phi(\omega)}, \; m = 0,1 \ldots M-2 \tag{B.8}$$

Substituting these values in (B.7) and (B.8) back into (B.4) allows us to write our final equation

$$|\Phi(\omega)|^2 = |\Phi(M\omega)|^2 + \sum_{m=0}^{M-2} |\Psi_m(M\omega)|^2 \tag{B.9}$$

Appendix C

Phase Response of M – Band Bandlimited Wavelets

Assume that there are M filters, $P_m(\omega)$, where $m \in \{0,1 \ldots M-1\}$ as defined by the magnitude solution in the above derivation. For all filters $P_n(\omega)$ and $P_m(\omega)$, only adjacent filters, |m-n|=1 where $m,n \in \{0,1 \ldots M-1\}$, have overlapping areas where the phase solution becomes critical. All other filters by their magnitude solutions are implicitly orthogonal to one another. For each neighboring filter pair we can index the regions of overlap with the quantity q where $q \in \{0,1 \ldots M-2\}$. Here q=0 indexes $P_0(\omega)$ and $P_1(\omega)$ overlap, q=1 indexes $P_1(\omega)$ and $P_2(\omega)$ overlap, and so forth up to q=M-2 which indexes $P_{M-2}(\omega)$ and $P_{M-1}(\omega)$ overlap.

For any given q, we define a new function $Q_q(\omega)$ as

$$Q_q(\omega) = P_q(\omega)P_{q+1}^*(\omega) \tag{C.1}$$

$Q_q(\omega)$ is 2π periodic and we need only concern ourselves with canceling over a single period, $-\pi < \omega \leq \pi$, to properly cancel all periods of the function. The form that $Q_q(\omega)$ takes is defined by the products of two neighboring filters. In a single period, this product results in two "humps" where the filters overlap. These humps will be centered and symmetric about the points

$$\pm \frac{(q+1)\pi}{M} \tag{C.2}$$

The symmetry is critical in the cancellation and is due to the relationships between $\gamma(\omega)$ and

$\tilde{\gamma}(\omega)$ that were used to define the scaling and wavelet filter FT's. From (4.59) we can write

$$\sum_{k=-\infty}^{\infty} Q_q\left(\omega + \frac{2\pi k}{M}\right) = 0 \qquad \textbf{(C.3)}$$

We start by assigning a phase of zero to the scaling filter, $P_0(\omega)$. It is then possible to assign a linear phase to $P_1(\omega)$ with respect to the phase of $P_0(\omega)$ that will provide for cancellation of the terms in (C.3). This process can then be iterated for each neighboring filter so that (C.3) is satisfied across all filters. Each assigned phase is with respect to the previous filters phase, which implies that the phase with respect to the scaling filter is accumulative.

Iterating equation (C.3) over various values of k shows that for each iteration the function $Q_q(\omega)$ is shifted by an amount $\frac{2\pi}{M}$. If we define a new function, $\rho_q(\omega)$, that when multiplied by the magnitude function, $|P_{q+1}(\omega)|$, results in assigning a phase to the filter without causing magnitude distortion, we can satisfy (C.3). This function will be defined by

$$\rho_q(\omega) = e^{-jz(q)\omega} \qquad \textbf{(C.4)}$$

The expression in (C.4) defines a function that has a unity magnitude and a phase defined by the function z(q). At this point we need to define the function z(q) to provide for proper cancellation.

For each $Q_q(\omega)$, equation (C.3) must be iterated q+1 times before the "humps" will overlap and provide us with an opportunity to cancel the phase. This will be valid for all q in which the center point of the "hump", $\tilde{\omega}_q$, satisfies

$$\left|\tilde{\omega}_q\right| < \frac{\pi}{2} \qquad \textbf{(C.5)}$$

The result in (C.5) is therefore valid over integer q where

$$0 \le q < \frac{M}{2} \tag{C.6}$$

Out side of this range,

$$\frac{M}{2} \le q \le M - 2 \tag{C.7}$$

the overlapping "humps" coincide with values in the next period of $Q_q(\omega)$. The equation in (C.3) must be then iterated M-(q+1) times for any

$$\left|\tilde{\omega}_q\right| \ge \frac{\pi}{2} \tag{C.8}$$

before the opportunity of cancellation can occur. In each of these two scenarios, when overlap occurs, we must have assigned a phase of exactly π to the shifted $Q_q(\omega)$ to force (C.3). We do this by assigning the phase of $P_{q+1}(\omega)$ such that the product in (C.1) has phase

$$\angle Q_q(\omega) = \angle P_q(\omega) - \angle P_{q+1}(\omega) = \angle P_q(\omega) - \left[\angle P_q(\omega) + \alpha\omega\right] = -z(q)\omega \tag{C.9}$$

The negative sign in (C.9) is a result of the complex conjugate in (C.1).

If we divide the unit circle, $e^{-j\omega}$, into M units we can determine the value that z(q) must take to provide for the cancellation in (C.3). As explained earlier there are two regions, those defined by (C.6) and (C.7), that we must concern ourselves with. For the first region we have (q+1) shifts before overlap occurs.

$$z\frac{2\pi(q+1)}{M} = \pi \tag{C.10}$$

Where z is a constant multiplier to provide for the proper resulting phase. Solving for z gives

$$z(q) = \frac{M}{2(q+1)} \tag{C.11}$$

In the second region we have M-(q+1) shifts before cancellation can occur. This implies that

$$z\left[\frac{2\pi(M-(q+1))}{M}\right]=\pi \tag{C.12}$$

Again solving for z we have

$$z(q)=\frac{M}{2(M-(q+1))} \tag{C.13}$$

The two expressions in (C.12) and (C.13) can be summarized as

$$z(q)=\begin{cases}\dfrac{M}{2(q+1)} & for \quad 0\le q<\dfrac{M}{2}\\ \dfrac{M}{2(M-(q+1))} & for \quad \dfrac{M}{2}\le q\le M-2\end{cases} \tag{C.14}$$

When substituted back into (C.4) this gives the proper relative phase between neighboring filters so that cancellation of overlapping regions can occur.

Bibliography

1. A.S. Bopardikar, R.M. Rao and B.S. Adiga, "PRCC Filter Banks, Matched Sampling Systems and Implementation of Bandlimited Discrete Wavelet Transform," *IEEE Transactions on Signal Processing*, August 2000.
2. J.O. Chapa and R.M. Rao, "Algorithms for Designing Wavelets to Match a Specified Signal," *IEEE Transactions on Signal Processing*, December 2000
3. P. Stedden, P.Heller, R. Gopinath, C. Burrus, "Theory of Regular M – Band Wavelet Basis" IEEE Trans on Signal Processing, DEC 1993 Vol. 41 pg 3497
4. W. W. Jones "A Unified Approach to Orthogonally Multiplexed Communications Using Wavelet Basis and Digital Filter Banks", Ph.D. dissertation, University of Ohio, Athens, Aug. 1994
5. T.D. Tran and T. Q. Nguyen, "On M-Channel linear Phase FIR Filter Banks and Application in Image Compression" IEEE Trans on Signal Processing, Vol. 45, pp 2175 Sept. 1997
6. T.Q. Nguyen and P.P. Vaidyanathan "Two channel PR QMR structures which yield linear-phase analysis and synthesis filters" IEEE Trans on Acoustics, Speech and Signal Processing Vol. 37, pp 676 May 1989
7. M. Vetterli and D. Le Gall, "Perfect-reconstruction filter banks: some properties and factorizations" IEEE Trans on Acoustic, Speech, and Signal Processing, Vol. 37 pp. 1057 July 1989

8. P. Saghizadeh and A.N. Willson Jr. "A generic approach to the design of M-channel uniform-band perfect-reconstruction linear Phase FIR Filter Banks" Proc. IEEE Int. Conf. On Acoustics, Speech, and Signal Processing pp. 1300 May 1995
9. P.P. Vaidyanathan "Quadrature Mirror Filter Banks, M – Band extensions and Perfect Reconstruction Techniques" IEEE Acoustics, Speech and Signal Processing Magazine pages 4-20 1987
10. P.P. Vaidyanathan "Multirate Digital Filters, Filter Banks, Polyphase Networks, and Applications: A Tutorial." IEEE Proceedings, 78:56-93 January 1990
11. M. Vetterli and C. Herkey. "Wavelets and Filter Banks: Theory and Design" IEEE, Trans on Acoustics, Speech and Signal Processing, pages 2207-2232, Sept 1992
12. M. J. Vetterli, "Multirate Filter Banks", IEEE Transactions on ASST, 35:356-372 1987
13. H. Zou and A. H. Tewdik. "Discrete Orthogonal M – Band Wavelet Decompositions." In Proceedings of ICASSP, San Francisco, CA Volume 4 Pages IV-605-IV608. IEEE 1992
14. S. Basu and H.M. Choi. "Linear Phase IIR Wavelets and Perfect Reconstruction Subband Coding." In Proc IEEE Int Conf Systems, Man and Cybernetics volume 4, Pages 507-512, Le Touquet, October 17-20 1993
15. L.L. Presti and G. Olmo "A Realizable Paraunitary Perfect Reconstruction QMF Bank Based on IIR Filters" Signal Processing, 49(2)133-143 March 1996

16. M.J.Smith "IIR Analysis / Synthesis System" In J.W. Woods, editor, Subband Image Coding, Pages 101-142, Kluwer Academic Publishers 1991

17. P.P. Vaidyanathan and P.Q. Hoang "Lattice Structures for Optimal Design and Robust Implementation of Two Channel Perfect Reconstruction QMF Banks", IEEE Trans on Acoustics, Speech and Signal Processing Vol. 36. No 1 pp.81-94 Jan 1988

18. M. Vetterli "Filter Banks Allowing for Perfect Reconstruction," Signal Processing, pp. 219-244 April 86

19. Vaidyanathan, P.P. "Theory and Design of M-Channel Maximally decimated Quadrature Mirror Filter with Arbitrary M, Having Perfect Reconstruction Property," IEEE Transaction on ASSO pp. 476-492 April 87

20. Nguyen, T. Q. and Vaidyanathan, P.P. "Two Channel Perfect Reconstruction FIR QMF Structures which Yield Linear Phase Analysis and Synthesis Filters", IEEE Trans on ASSP pp. 676-690 May 1989

21. Soman, A.K., Vaidyanathan, P.P. and Nguyen, T.Q., "Linear-Phase Paraunitary Filter Banks; Theory, Factorizations and Applications," IEEE Trans. On SP Vol. 41 Dec 1993

22. T.E.Tuncer and T.Q. Nguyen, "General Analysis of Two – Band QMF Banks," IEEE Trans on Signal Processing Feb 1995

23. Kiya H. Yae M. and Iwahashi, M., "A Linear-phase Two-channel filter bank allowing perfect reconstruction" Proc IEEE ISCAS pp 951-954 1992

24. Vaidyanathan, P.P. Regalia, P and Mitra, S.K., "Design of doubly complementary IIR Digital Filters using a Single Complex Allpass Filter, with Multirate Applications." IEEE Trans on Circuits and Systems, pp. 378-389 April 87

25. Ekanayake, M. M. and Premaratne, K., "Two Channel IIR QMF Banks with approximately linear-phase analysis and synthesis filters" Proc of 28th annual asilomar conference, Nov 94

26. T.Q. Nguyen, T.I. Laakso and T.E. Tuncer, "On Perfect-Reconstruction Allpass-Based Cosine Modulated IIR Filter Banks", Proceeding of ISCAS 94, pp.2-33 2-36

27. Y. Meyer, "Wavelets: Algorithms and Applications," Philadelphia : SIAM, 1993

28. J. Huang and G. Gu, "A direct approach to the design of QMF banks via frequency domain optimizations," IEEE Trans. Signal Processing, vol. 46, 2131-2138, Aug. 1998.

29. T. Tran, R. de Queiroz and T. Q. Nguyen, "Linear-Phase Perfect Reconstruction Filter Bank: Lattice Structure, Design, and Application in Image Coding" IEEE Tran on Signal Processing, vol. 48, no. 1, January 2000

30. T. Q. Nguyen and Vaidyanathan, P.P, "Structures for Perfect Reconstruction FIR QMF Banks which Yield Linear Phase Analysis Filters," IEEE Transactions on ASSP Vol. 38 No. 3 March 1990

31. W. W. Jones and J. C. Dill, "The Square Root Raised Cosine Wavelet and its Relation to the Meyer Functions" IEEE Transactions on Signal Processing, Vol. 49 No. 1, Jan 2001

32. N. El-Boghdadly and N. Sadek, "Design of Scaling and Wavelet filters as FIR AND IIR QMF Filters and their Applications," Fifteenth National Radio science Conference C18 1, Feb 24 1998

33. I. Selesnick, "Formulas for Orthogonal IIR Wavelet Filters" IEEE Transactions on Signal Processing, Vol. 46, No. 4, April 1998

34. T. Q. Nguyen, R.D. Koilpillai, "The Theory and Design of Arbitrary Length Cosine-Modulated Filter Banks and Wavelets, Satisfying Perfect Reconstruction" IEEE Transactions on Signal Processing Vol. 44, No. 3, March 1996

35. Truong Q. Nguyen. "A Tutorial on Filter Banks and Wavelets", 1995.

36. X. Gao, T.Q. Nguyen, G. Strang, "On Factorization of M-Channel Paraunitary Filterbanks", IEEE Transactions on Signal Processing, Vol. 49, No. 7, July 2001

37. G.G. Walter, J. Zhang, "Orthonormal Wavelets with Simple Closed-Form Solutions" IEEE Transactions on Signal Processing, Vol. 46, No. 8 August 1998

38. S. Mallat, "A Theory for Muliresolution signal Decomposition: The Wavelet Representation," IEEE transactions on Pattern Analysis and Machine Intelligence, Vol. 11, No. 7, July1989

39. I. Daubechies, Ten Lectures on Wavelets, Society for Industrial & Applied Mathematics, 1992

40. Y. Meyer, Wavelets and Operators, Cambridge University Press, 1995

41. R. M. Rao, A.S. Bopardikar, Wavelet Transforms : Introduction to Theory and Applications, Addison Wesley, 1998

42. M. Vetterli, J. Kovacevic, Wavelets and Subband Coding, Prentice Hall 1995

43. C. S. Burrus (Contributor), R.A. Gopinath, H. Guo, Introduction to Wavelets and Wavelet Transforms: A Primer, Prentice Hall 1997

44. R. W. Hamming, Digital Filters, Dover Publications, 1998

45. John G. Proakis, Dimitris G. Manolakis, Digital Signal Processing Principles, Algorithms and Applications, Prentice Hall, 1996

46. P. P. Vaidyanathan, Multirate Systems and Filter Banks, Prentice Hall, 1992

47. K. Sayood, Introduction to Data Compression, Second Edition, Morgan Kaufmann Publishers, 2000